化學機械研磨機台製程設備模擬器及控制器之設計與實作

學生：陳鼎銘　　　　　　　　　　　　　　指導教授：林家瑞　博士

國立交通大學機械工程學系

碩士論文

摘要

本論文主要目的在利用實體迴路(Hardware In the Loop, HIL)的概念，針對半導體製程中的化學機械研磨機台(Chemical Mechanical Polishing, CMP)，設計一套包含模擬器與控制器的平台。研究重點在於利用兩台獨立的工業電腦來設計CMP系統的模擬器與控制器，並以Windows XP及 Window 2000 為發展平台，Matlab、BC++ Builder為開發工具，來完成此一架構。

論文中說明化學機械研磨機台的基本架構和主要參數，同時介紹 Run To Run EWMA (Exponentially Weighted Moving Average)及 FNN (Fuzzy Neural Network)控制模式，建構應用於化學機械研磨的單元控制器，並利用 RS-232 硬體介面來建構通訊模組將數據回傳做迴饋控制，經由修正製程設備控制系統的控制參數改善其功效。

Development of simulator and control system for CMP process equipment

Student：Ting-Ming Chen Advisor：Dr. Chia-Shui Lin

Department of Mechanical Engineering

National Chiao Tung University

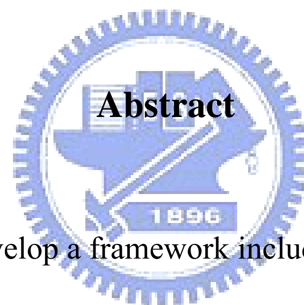

Abstract

In this thesis, we will develop a framework including simulator and controller for the Chemical Mechanical Polishing (CMP) equipment in the semiconductor industry by using the concept of Hardware-In-the-Loop (HIL). We use two independent computers to design simulator and controller for CMP process and adopt Matlab、BC++ Builder as the developing tools implemented on the Windows XP and Window 2000 platform.

We explain the basic architecture and the primary parameters for the CMP equipment. We also introduce Run to Run EWMA (Exponentially Weighted Moving Average) and FNN (Fuzzy Neural Network) concept to establish the controller for CMP process and use RS-232 hardware to build the communication module to pass the data back and forth for feedback control. As a result, the control system can be used to continuously improve the performance of the control system.

誌謝

這兩年的研究所生活中，體驗到許多人生的經驗，也見識到什麼叫求學的態度，令我受益良多。實在非常感謝身邊許許多多幫助過我的人，讓我能從懵懵懂懂的境界裡，漸漸的了解如何面對問題、如何分析問題，甚至到具備處理問題的能力。首先感謝林家瑞 教授的指導並給予我一個非常大的空間發揮，讓我懂的從不同的角度去分析解決每一件事情。再來要感謝建宇 學長和俊霖 學長對我的協助及幫忙，解決我在研究方面許多的困惑。當然這兩年來同期同學的鼓勵和陪伴更是我能順利完成學業的原動力，尤其是文志和峰龍在修課上的協助以及淦垚和劭恩在程式方面的指導，讓我在課業上都能迎刃而解。我想，這兩年的生活裡要感謝的人實在太多，每一件發生在我身上的事，每一個我遇到的人，對我來說都是非常珍貴和美麗的。再一次由衷的感謝為我譜寫這值得回憶的每一個人。

Table of Contents

Chinese Abstract……………..………………………………………………….. Ⅰ

English Abstract……………………….………………………………………Ⅱ

Acknowledgement………………………………………………..………………Ⅲ

List of Figures……………………………………………………………………Ⅵ

List of Tables……………………………………………...………………Ⅸ

Chapter 1 Introduction……………..1

1.1 Motivation..1

1.2 Literature Survey...3

1.3 Objective of the Research…………………..………………………………..6

1.4 Thesis Outline……………………………………………………………...7

Chapter 2 Chemical Mechanical Planarization – An Introduction……………….8

2.1 Development of CMP……………………………………………………...8

2.2 Introduction of CMP Structure……………………...…………………………9

2.3 CMP Process Parameters………………………………………………...11

2.3.1 Mechanical Parameters……………………………………………11

2.3.2 Chemical Parameters………………………………………………...13

2.4 Model of Chemical Mechanical Planarization…………………………...14

2.4.1 Preston Equation…………………………………………………….15

2.4.2 Luo and Dornfeld Equation……………………………………….15

Chapter 3 Run-to-Run Control Law…………………………….…………….……..17

3.1 Introduction of Run-to-Run control…………………………………...…17

3.2 History of the Development of Run-to-Run Control….………...……….…18

3.3 EWMA based Run-to-Run Control System……………………...…………19

3.4 Fuzzy Neural Network based Run-to-Run Control System……..……….…22

3.4.1 Radial Basis Function based Fuzzy Neural Network ……….……..22

3.4.2 The Training of the Network……………………….….…………24

3.4.3 The Concept of Zero Error Tracking Control……………….……….27

Chapter 4 Simulation and Analysis for CMP Controller……………...…..………31

4.1 Simulations using Preston Equation for SiO2 CMP Process……..…..……31

4.1.1 EWMA controller for Preston Equation…………………...……...31

4.1.2 Zero Error Tracking Fuzzy-Neural Network Controller for Preston Equation…………………………..…………………....……32

4.1.3 Comparison of Simulation Results……………………….............33

4.2 Simulations using Luo and Dornfeld Equation for Copper CMP Process….34

4.2.1 EWMA Controller for Luo and Dornfeld Equation……..…………..34

4.2.2 Zero Error Tracking Fuzzy-Neural Network Controller for Luo and Dornfeld Equation…………………………...………………...35

4.2.3 Comparison of Simulation Results ……………….……………36

4.3 Summary of Simulations…………………………………………...……36

Chapter 5 Run-To-Run Controller Implementation……………………….……..37

5.1 Hardware and Module Descriptions…………………………………...37

5.2 Program Design Flow…………………………………………………38

5.3 Introduction of Run-To-Run Operator Process Interface………………..…40

5.4 Summary and Contribution....………………..……………………………..42

Chapter 6 Conclusion and Future Work……………………………….………44

Reference……………………………………………………………………………72

ES 1896

List of Figures

Figure 1.1 Hierarchical control structure [2]……………………………………46

Figure 1.2 The control structure for CMP equipment……………………...…46

Figure 2.1 The mimic schematic of CMP equipment [9]……………….……47

Figure 3.1 R2R control diagram [22]………………………………….….…47

Figure 3.2 The relationship between input and output of R2R controller [22]….48

Figure 3.3 CMP R2R process control strategy [13]…………………………..48

Figure 3.4 EWMA R2R control block diagram……….………………………...49

Figure 3.5 Fuzzy Neural Network (FNN) structure…………….……………49

Figure 3.6 Radial basis function based Fuzzy Neural Network (FNN) structure ……………………………………………………………………50

Figure 3.7 The curve of membership function (m=5， α=1.2， β=8.5)………50

Figure 3.8 Zero error tracking Fuzzy Neural Network (FNN) control block diagram……………………………………………………………………51

Figure 4.1 Simulation of removal rate variation by Preston Equation……..…….51

Figure 4.2 Comparisons between the outputs of Preston equation and EWMA predictor……………………………………………………………..52

Figure 4.3 Control result of EWMA R2R controller…………….……………52

Figure 4.4 The input variation of EWMA R2R controller………………………53

Figure 4.5 The predictive error of each run in EWMA predictor………………..53

Figure 4.6 Comparisons between the outputs of Preston equation and rough tuning of FNN predictor…………...………………………………54

Figure 4.7 The error decreasing trend of fine tuning FNN predictor……………54

Figure 4.8 Comparisons between the outputs of Preston equation and fine tuning FNN predictor…………………………………………………………55

Figure 4.9 Control result of zero error tracking FNN controller………………...55

Figure 4.10 The input variation of zero error tracking FNN controller………...56
Figure 4.11 Simulation data of removal rate variation by Luo and Dornfeld Equation……………….……………………………………….….56
Figure 4.12 Comparisons between the outputs of Luo and Dornfeld equation and EWMA predictor……………………………...………………57
Figure 4.13 Control result of EWMA R2R controller…………………………...57
Figure 4.14 The input variation of EWMA R2R controller……………….…….58
Figure 4.15 The predictive error of each run in EWMA predictor………………58
Figure 4.16 Comparisons between the outputs of Preston equation and rough tuning FNN predictor……………………………………………59
Figure 4.17 The error decreasing trend of fine tuning FNN predictor…………..59
Figure 4.18 Comparisons between the outputs of Preston equation and fine tuning FNN predictor…………………………..…………….……60
Figure 4.19 Control result of zero error tracking FNN controller……………….60
Figure 4.20 The input variation of zero error tracking FNN controller………...61
Figure 5.1 EES Box [29]………………..……………………………….….61
Figure 5.2 The framework of simulator and controller…………………..….…62
Figure 5.3 Program design flowchart of Simulation Run Mode (Controller)….62
Figure 5.4 Program design flowchart of Simulation Run Mode (Simulator)…..63
Figure 5.5 Program design flowchart of R2R Control Mode…………..………63
Figure 5.6 The Operator Process Interface (OPI) of the controller……..…..…64
Figure 5.7 The Simulator of CMP Process Equipment…………………..…….64
Figure 5.8 The enter frame of the controller…………………..……………65
Figure 5.9 The Simulation Run Mode……………..…………………………...65
Figure 5.10 The “Result” section of Simulation Run Mode (Controller)……….66
Figure 5.11 The “Result” section of Simulation Run Mode (Simulator)………..66

Figure 5.12 The current plots of Simulation Run Mode…………………………...67

Figure 5.13 Export data…………………………………………………………….....67

Figure 5.14 The R2R Control Mode………………………………………….……68

Figure 5.15 The current plots of R2R Control Mode……………………………68

List of Tables

Table 2.1 Advantages of CMP [18]…………………………………..……….69

Table 2-2 The Parameters of CMP Process [18]………………………………...70

Table 5.1 The specification for the EES Box [29]………………………………71

Chapter 1

Introduction

The chemical mechanical polishing (CMP) process has been widely accepted in the semiconductor industry for oxide dielectric and metal layer planarization. Control of the CMP process is an active research area in both academia and industry. Due to the fact that the CMP process is not completely understood and there is a lack of in- situ sensors, and real-time control of the CMP process is difficult. As a result, run-to-run control strategies are used to monitor CMP process. Nowadays, many semiconductor manufacturers have made a lot of efforts in developing all kinds of solutions to overcome the process variation in order to get an advantageous position in the semiconductor industry.

1.1 Motivation

The semiconductor industry has already moved towards the development of 100 nm technology node at present. First of all, the throughput becomes a very key indicator on how to improve the yield of the equipment and overall equipment effectiveness. Secondly, reduction of the broken wafer is another key point to decrease the production costs and to improve products quality. In order to enhance the processes that we mention above, the Integrated-Circuit (IC) manufacturers and the equipment vendors spend a lot of resources to research the operation technique and the improvement of equipment performance. Advanced Process Control (APC) is becoming a critical component to improve performance, yield, throughput, and flexibility of the manufacturing process using run-to-run, wafer-to-wafer, within

wafer and real-time process control. It includes Real-Time Monitoring and Control System 、 Fault Detection and Classification (FDC) 、 Feedback/Feedforword Run-to-Run Control and Predictive Maintenance abilities that can help the engineers to reduce down time, to detect and eliminate the failure rates of process equipments, and to compensate various disturbance (such as process shift ,drift and variance) by means of modifying the process recipes. It is useful for enhancing the yield and the quality of the products [1] [3].

According to the results we mention above, the industry starts to develop a control strategy that supports control and optimization for fab-wide goals (such as yield) through the coordinated control of individual process parameters. The strategy that is generally being adopted breaks apart the control problem into layers, resulting in a hierarchical control structure as depicted in Fig. 1.1. In this illustration, the factory is divided into three layers: process, measurement, and control. The control layer is further subdivided into process, interprocess, and factory-level sublayers. At the lowest control layer, standard R2R control solutions use feedforward and feedback data to provide control of process quality parameters, such as CMP film thickness, to specified targets. FDC is used to determine if the tool is in acceptable condition where control should be applied, and further serves to filter data into the controllers. At the intermediate control layer, interprocess control solutions coordinate groups of process controllers to achieve multiprocess targets. An example here is CD control coordinated between lithography and etch process steps [2].

Because the equipments of the semiconductor industry are very expensive, it is necessary to simulate the process to avoid making damage of equipments in advance. Therefore we use two independent computers to design simulator and controller by the concept of Hardware In the Loop (HIL). One of the computers is the simulator.

It receives the control signal and calculates the change of the removal rate before it outputs the signal of the removal rate. The other computer is the controller of the removal rate. It can receive the output signal from simulator and attempt to control the simulator. We use Preston equation and Luo & Dornfeld equation as the process models in the simulator and design the controller to control the simulator, hence we can test the performance in advance. In order to simulate the realistic case, it models the control and feedback signals in the tow computers and test one controller in this interactive simulation. We can develop the realistic CMP machine controller in the future before we remove the simulator to achieve Run-to-Run control [4].

1.2 Literature Survey

Hardware In the Loop (HIL) is a powerful method for testing system components such as control system electronics without connection to the real equipment under control. The increasing adoption of HIL has been driven by a number of factors, including the ability to perform system testing before the complete system is available and to simulate failure conditions which would be dangerous or expensive to perform on the real plant. It is an important tool for reducing development time and ensuring safety and reliability of components with complex behavior [5] [6].

When the hardware has not be established, the hardware designer makes efforts in developing the equipment on one hand, and the software designer realizes controller and simulator simultaneously on the other hand in order to develop the equipment efficiently. But the software would be accomplished first, and then the software engineer could test and verify the controller by the simulator first. Capturing the realism of industrial control problems requires a complex installation or machinery, both costly and inflexible, in some cases potentially dangerous for the

engineers. Therefore, it is suggested to have the optimal control performance via testing and tuning the controller before connecting to the real hardware to avoid dangerous and costly mistakes like equipment failure. The purpose of this configuration is to make the hardware component behave as closely as possible to what would be encountered in the real world.

The software verification method is done by connecting the controller output signal to the input of the simulator and connecting the output signal of the simulator to the input of the controller. By the way, the equipment could be replaced by the simulator to verify the processes in advance [7] [8].

The most important part of the controller design is to learn thoroughly about the process to be controlled. Besides experimental data, it is also very helpful to establish the model of CMP removal rate. Based on the fact that the mathematics model is very complicated for the plant to design its controller. We need to simplify it and take out the representative part usually. This process of using the simplified mathematical model to design the controller generates mode-based control system.

Run-to-run control is a methodology to improve manufacturing performance for processes subject to disturbance and becoming increasingly important in the semiconductor industry. The key characteristic of the run-to-run approach is that the feedback concept of the automatic process control is brought into the statistical process control. The quality of the previous product or previous batches of products is used to analyze current process status (shifting or drifting). The tendency of the system's performance is predicted by a forecast algorithm. Based on this forecasting, modifications can be made to the process parameters to compensate for losses in performance. Advantages of the run-to-run control scheme can be mentioned as follows [9]: (1) no additional on-line sensor is required, (2) a non-standard process is applicable, (3) the process monitoring task can be accordingly executed.

Sachs is the first one who applies EWMA (Exponentially Weighted Moving Average) to the Run-to-run control in the semiconductor industry [10]. Chen and Guo then presented an aged-based double EWMA scheme for the CMP process to accommodate process drifts and noises [11]. A concept of " sheet film equivalent " (SFE) was used to design a R2R CMP control scheme for dielectric application, and the experimental results from Texas Instrument fab were compared with the EWMA control scheme [12]. The scenario is developed for the linear chemical-mechanical planarization process. The controlled CMP process parameters could be belt speed, head speed, slurry rate, conditioner pressure, etc., and the process responses are material removal rate, wafer nonuniformity, and planarization, etc. EWMA model was used to design removal rate and uniformity controller in CMP process [13]. It becomes the most popular linear model-based controller for process control engineers in semiconductor industry.

The investigation of additional run-to-run control methods appears fruitful, potentially including classical LQG, neural network, or stochastic dynamic programming approaches that can take full advantage of emerging empirical and physical models of the process (particularly those incorporating process dynamics). Lin and Liu [14] used an adaptive neuro-fuzzy interface system to analyze CMP process parameters on rotary CMP tools. The objective is to investigate the use of neural networks to model and control the polishing uniformity of the linear CMP process [15].

An object-oriented programming (OOP) environment to develop SEMI Equipment Communication Standard (SECS) using the C++ and C programming languages in a Unix workstation environment is described. The system defines a set of programming objects corresponding to the standard SECS-II item types, messages and headers as well as a number of support classes and operations. Conversion

between standard program datatypes and SECS-Ⅱ items is transparent or explicitly managed by the developer. Within a standard framework using standard C++ input/output methods, SECS-Ⅱ messages may be created, analyzed, transmitted and received between internal buffers, external files and communication channels. Classes corresponding to specific SECS stream and function codes are also available and can be incorporated easily into application code with little or no modification [16] [23].

1.3 Objective of the Research

In this thesis, we aim at developing a framework including simulator and controller for the Chemical Mechanical Polishing (CMP) equipment. We use two independent computers to design simulator and controller for CMP process and BC++ Builder as the developing tools implemented on the Windows XP platform. We also use RS-232 hardware to build the communication module to simulate the signal interactions of the real machine as shown in Fig. 1.2.

Preston equation [20] and Luo and Dornfeld equation [21] will be adopted as the mathematical models of CMP process in the simulator computer. EWMA and Neural Network algorithm will be used in the controller computer. By using the concept of run-to-run control, the frame of CMP process control will be established and via the feedback control law the control system can continuously adjust the control parameters for the control system to improve performance of the controller. As a result, the various disturbances, such as process shift, drift and variance will be compensated and corrected. Because of the control signals between the two computers are simulated as in the real situation, we hope that we can develop the CMP control system by this concept in the future.

1.4 Thesis Outline

This thesis is organized as follows. In chapter 1, we introduce the concept and motivation to accomplish the objective of research. In chapter 2, we describe the structure and the main parameters of CMP equipment. In chapter 3, we discuss the development and concept of run-to-run control, and establish the controller by way of EWMA and Fuzzy Neural Network. Simulation results of EWMA and Fuzzy Neural Network based modeling and control of CMP process are discussed in chapter 4. In chapter5, we illustrate how to implement the controllers and plants by two computers individually. Concluding remarks and future work are given in chapter 6.

Chapter 2

Chemical Mechanical Planarization – An Introduction

Planarization is the process of smoothing of the material surfaces. Chemical mechanical planarization (CMP) is the process of smoothing of the material surfaces aided by the chemical and mechanical forces. CMP also refers to chemical mechanical planarization that causes planarization of material surfaces. Note, however, that polishing and planarization are not synonyms. Polishing generally refers to smoothing of material surfaces not necessarily planarization of material surfaces. Here we shall use CMP for chemical mechanical planarization [18].

2.1 Development of CMP

E S A
1896

Historically CMP has been used to polish a variety of materials for thousands of year, for example to produce optically flat and mirror finished surfaces. Nature has run its own CMP process to produce beautifully finished stones, finishing affected by year of exposure to generally not-so-aggressive chemical and mechanical forces. Beautifully finished inlaid metal objects have been prepared by the so-called “damascene” process. More recently optically flat and damage-free glass and semiconductor surfaces have been prepared by the use of the CMP processes. Now CMP process is being introduced in planarization of the interlayer dielectric (ILD) and metal layers used to form interconnections between devices and the real world outside of IC. It is projected that the observed effectiveness of the CMP process will lead to the widespread use of this process at various stages of integrated circuit (IC) fabrication, for a variety of high performance and application-specific ICs, and for a

variety of materials [18].

As the feature size of devices move from sub-0.25 μm to sub-0.10 μm regime and the number of multi-layered structures increases, atomically flat surfaces are needed in manufacturing the interconnects of microelectronic devices. The growth of the CMP process is associated with the effectiveness in improving the yield and performance of the circuits in many different applications. Increasing the operational time, decreasing the scale design, and increasing the number of metal/dielectric layer on the IC chips are three main goals in semiconductor industries. Improving the CMP process will in fact achieve these goals.

Table 2.1 [18] lists several advantages of CMP. The most important advantage is that CMP achieves globally planarization which is essential in building multilevel interconnections.

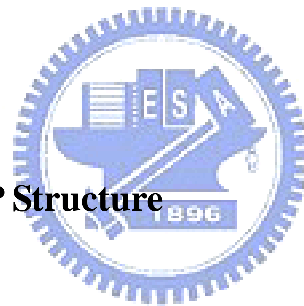

2.2 Introduction of CMP Structure

The Chemical Mechanical Polishing (CMP) process is critical to current and future generation of integrated circuits due to its ability to achieve global planarization, which is essential for multilevel interconnects. The CMP process involves a patterned silicon wafer, attached to a carrier by vacuum, pressed face down into a polishing pad. The polishing environment is flooded with a colloidal slurry which physically enhances abrasion and helps prevent redeposition of oxide or metal. The polish table is rotated while the wafer also is rotated about their axes and orbits about the polish table. The goal of planarization process is to produce wafers which are as flat as possible for a targeted thickness within a surface uniformity tolerance [17]. A schematic of a CMP equipment is shown in Fig. 2.1 [9]. The primary segments of CMP machine are as follows：

(1) Wafer Carrier：

The wafer carrier holds the wafer face down during CMP and brings the wafer in contact with the polishing pad. The carrier rotates in the same direction as the platen.

(2) Platen：

The rotating base on which the polishing pads are placed. Sometimes referred to as the polishing "table".

(3) Pad：

A pad which is mounted on a rotating platen and polishes the wafer. Polishing pads come in a variety of materials and are designed with a variety of surface features depending on the process results needed. Pad conditioning is a process in which the polishing pad is "roughed up" by a diamond disc in order to reduce the effects of glazing. The pad conditioning can enhance pad performance, but reduces overall pad lifetime.

(4) Slurry：

An abrasive mixture containing particles of colloidal silica, alumina, or some other abrasive material suspended in a chemical compound and DI water. Slurry is fed onto and through the polishing pad during CMP in order to remove material from the wafer surface.

If we only care about the amount of mechanical abrasion, it will result in a decreased removal rate and the wafer surface may peel off or be scratched. On the

other hand, if we only care abut the amount of chemical reaction removal, it will lead to the erosion of the dielectric or the dishing of the metal lines. Giving undue emphasis to either of them will not achieve the global planarization. Therefore, how to combine the mechanical abrasion and chemical reaction to get good performance and high throughput is nowadays an important challenge to be dealt with [19].

2.3 CMP Process Parameters

As named chemical mechanical polishing, the primary parameters are divided into two parts which are the chemical aspect and the mechanical aspect.

2.3.1 Mechanical Parameters

The primary mechanical parameters are as follows：

(1) Platen Speed：

The platen speed affects slurry transport across the wafer and the transport of the reactions and products of chemical reactions to and from the wafer surface. It has been noted that the copper removal rate is strongly dependent on the platen speed.

(2) Carrier Speed：

When the carrier speed is the same as the platen speed, the best uniformity will be achieved.

(3) Down Force：

As the down force increases, the removal rate increases and then reduces the polishing time. This, of course, means higher throughput. The danger is that too much down force can cause problems such as scratches or gouges, and can possibly cause non-uniformity.

(4) Back Pressure：

It is sometimes used to provide some curvature or shape to the wafer during polishing. The idea is to produce an optimum wafer shape with respect to the pad underneath for improving removal rate distribution on the wafer and within-wafer-uniformity (WIWUN).

(5) Pad Conditioning：

There are variables which will affect pad conditioning. For instance, the conditioning duration, the abrasiveness of the disc and down force will all have an effect on the pad. A long conditioning duration may improve pad performance, but ultimately will reduce pad lifetime.

(6) Slurry Flow Rate：

Slurry flow rate affects how quickly new chemicals and abrasive are delivered to the pad and reaction by-products and used abrasive are removed from pad. It also affects how much slurry is on the pad and therefore will affect the lubrication properties of the system.

Furthermore, there are still other mechanical parameters which affect the process：polish oscillation, wafer mounting and pad hardness, for instance [19].

2.3.2 Chemical Parameters

The primary chemical parameters are as follows：

(1) Abrasive Size, Units of (nm)

Abrasive size affects the removal rate and the surface damage. In addition the distribution of abrasive size has a dramatic effect on surface damage.

(2) Abrasive Concentration, Units of weight percent, wt% in liquid volume

Generally, higher abrasive concentration leads to higher polish rate.

(3) Abrasive Variety

Silica oxide (SiO_2) is the most common used for oxide polishing while aluminum oxide (Al_2O_3) is the most common used for metal polishing.

(4) Slurry Viscosity

The more viscous a material, the more it resists flow. High slurry viscosity results in poor transport of reactants and products to and from the wafer surface. It also affects lubrication of the wafer pad interface.

(5) Oxidizers

For metal CMP, most of the chemical reactions are electrochemical in nature. Oxidizers react with metal surfaces to raise the oxidation state of the metal via a reduction-oxidation reaction, resulting in either dissolution of the metal or the formation of a surface film on the metal. For both tungsten and copper, polish has been shown to be proportional to the rate of these reduction-oxidation

reactions [18].

Furthermore, there are still other chemical parameters which affect the process： slurry temperature, slurry buffering and film hardness, for instance.

There are many variables that can affect the CMP performance as shown in Table 2-2. Besides, some factors which are difficult to control and monitor like the slurry transport under the wafer and the local temperature of the slurry also have significant effects on the CMP performance and the process parameters are interrelated such that modifications to one parameter will have an impact on other process issues. For instance, increasing platen speed or down force may increase the removal rate, yet at the same time create slurry flow rate and distribution problems. Therefore, the key problem is how to optimize the process parameter settings in order to obtain the desired results for the given film being planarized [19].

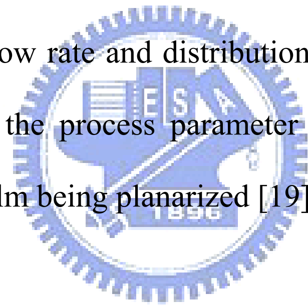

2.4 Model of Chemical Mechanical Planarization

The material removal model for CMP can be separated into two parts, mechanical model and chemical model. The chemical action of the slurry is responsible for continuously softening the silicon oxide or oxidizing the metal surface to form a thin passive layer which is immediately removed by the action of the slurry abrasives. The fresh silicon oxide or metal surface exposed due to the abrasion is then rapidly repassivated and removed. This process of passivation-abrasion-repassivation continues until the desired thickness is realized. Based on this idea, a mechanical removal model and a chemical model can be independently developed for CMP, with the mechanical model considering only the

mechanical removal of the passivation layer, and t he chemical model considering only the passivation of this layer [19].

2.4.1 Preston Equation

Preston provided a simple model of material removal in glass polishing tools, postulated based on experimental observation that the removal rate is proportional to the nominal applied pressure and the relative velocity between the pad and the material being polished. Preston equation [20] for the removal rate RR can be written as

$$RR = K_p P V$$

where P is the down pressure, V the relative velocity of wafer, and K_p a constant representing the effect of other remaining parameters, such as the abrasive type and concentration, and the nature of the chemicals and their concentrations. This equation has been widely used in CMP process control and consumable development for IC fabrication and manufacturing. However, it is focused on mechanical removal of material and there are some other phenomenons that can not be explained. For example, experimental results show that the pressure dependence of removal rate for CMP with soft pad satisfies a nonlinear relationship. Therefore, what is included in the all-purpose parameter K_p is unclear [19].

2.4.2 Luo and Dornfeld Equation

Luo and Dornfeld proposed a model to describe the interactions between the wafer, pad, and abrasives, which are quite different from those in conventional polishing or lapping processes due to the small pad hardness and different size scales

of the pad asperity and the polishing abrasives. They assumed the removal mechanism in the solid-solid contact mode instead of the hydro-dynamic mode. Luo and Dornfeld equation [21] for the removal rate RR can be written as

$$RR = C_2\left(1-\Phi\left[3-C_1P_0^{1/3}\right]\right)\sqrt{P_0}V + RR_C$$

where

P_0 is the down pressure

V is the relative velocity of wafer

C_1 is a constant representing the effect of slurry abrasives (average size and size distribution), wafer and pad hardness, and pad roughness

C_2 is a constant representing the effect of slurry chemicals, slurry abrasives, wafer size, wafer density, wafer hardness, pad material, and pad roughness

Φ is the normal cumulative distribution function which representing the probability density of active abrasives over the wafer-pad interface

$$\Phi(x) = \frac{1}{\sqrt{2\pi}}\int_{-\infty}^{x} e^{-(1/2)t^2}\,dt$$

RR_C is the material removal due to chemical etch

The values, C_1 and C_2, are independent of the down pressure P_0 and the relative velocity V. This model primarily is also focused on mechanical effect, particularly the abrasion due to the abrasive-wafer and abrasive-pad contact, but it includes the chemical reaction at the wafer surface. Therefore, this model looks more comprehensive to describe the CMP process.

According to Lee's thesis [19], the measured etching rate is quite small compared to the overall removal rate in the copper process. Therefore the chemical etching rate can be omitted and the equation will be adopted in the study as follow.

$$RR = C_2\left(1-\Phi\left[3-C_1P_0^{1/3}\right]\right)\sqrt{P_0}V \quad [19]$$

Chapter 3

Run-to-Run Control Law

To illustrate the benefits of advanced process control, the concept of the run-to-run control law is described briefly in this chapter. The control approach of EWMA and Fuzzy-neural network based run-to-run control systems are also described in this chapter.

3.1 Introduction of Run-to-Run control

Run-to-run control (R2R) is a control method for processes and equipments to compensate various disturbances, such as process shift, drift and variance, by means of modifying the process recipe. The typical run-to-run control block diagram is shown as Fig. 3.1. Following the previous block Metrology (Process N-1), the wafer enters the equipment (Process N). At the meantime, the result data from the metrology transfers to the controller (Process N) and is utilized as the tuning basis for the recipe (Process N). Such kind of control method is called feed-forward control. Another type of control method is called feedback control. It begins with the wafer at Equipment (Process N) entering Metrology (Process N). Next, the result data of Metrology (Process N) is fed back to Controller (Process N) and is also utilized as the tuning basis for the receipt (Process N).

The feed-forward control utilized the result data of metrology to determine the starting point of the process for the controller; and feedback control utilized the result data of metrology to determine the end point of the process for the controller. If the controller part is viewed individually, the relationship between the input and the

output can be shown as Fig. 3.2. Run-to-run control would compare the process recipe of specific process in the equipment with the results of upstream processes and downstream processes and then suggests the optimal recipe (or the correction of the process recipe) [22].

3.2 History of the Development of Run-to-Run Control

Continuous feature size reduction and wafer size increase have forced the players in the semiconductor industry to innovate to remain competitive. These innovations, for the most part, could be characterized as process-centric; that is, a specific tool and/or its specific process improved with the expectation that it will lead to improvement in overall factory throughput and yield.

In the mid-1980s, the predominant mechanism used in the industry (and to this day) is statistical process control (SPC). SPC is a method for detection of statistically significant data patterns based on an assumption of a Gaussian distribution of data. Mean and variance parameters are determined for various data parameters through data collection and analysis. The sensory data are then monitored with respect to these mean and variance parameters and alarm events are generated. While SPC is useful to detect and verify process stability and correctness, it is not technically a "control" solution. This is because SPC provides a mechanism for detecting aberrations but does not include mechanisms to correct for these aberrations.

In the late 1980s and early 1990s, researchers in the industry began to complement sensory and metrology research with a focus on utilizing the data to suggest correction. This effort named "advanced process control" (APC). However, the lack of adequate (especially in situ) sensing in semiconductor

manufacturing provided control systems researchers with unique challenges and opportunities for advancement. The first innovations in semiconductor manufacturing APC were the partitioning of the controlled process into the in situ control of the equipment environment, the in situ control of the equipment environment operating on the wafer, and the ex situ control of the final product for that process. This gives a hierarchical, nested partitioning of the control problem. With the industry accepting the hierarchical nested control solutions approach, research and development could now be focused on a particular level of control. Terminology somewhat specific to the industry was attached to each of these control levels. In-situ process environment and wafer environment control were collectively termed real-time, in situ, or time-critical control, while ex situ process control was termed run-to-run (R2R) control. In partitioning the control problem and control research, it became clear very quickly that, due to the available sensing capability and process knowledge, R2R control represented the first primary area where process improvements could be readily achieved [24].

3.3 EWMA based Run-to-Run Control System

The run-to-run control scheme was initially addressed by Sachs et al. [10] and the common example used is in chemical mechanical planarization process as shown in Fig. 3.3 [13]. The reaction of CMP process involves with complex mutual interaction between chemical and mechanical factors. Therefore parameters must be tuned and decided more carefully to obtain the optimal recipe. Boning et al. who used the exponentially weighted moving average (EWMA) controller to be the controller to adjust the removal rate and uniformity [13].

EWMA R2R controller is composed by a first order linear predictive model, a

EWMA filter and a controller, where the predictive model is obtained by the method of linear regression. Fig 3.4 represents the EWMA R2R control block diagram. First, we utilize the parameter of the previous t-1 (x_{t-1}) sampling run as the process input to obtain the current process output (y_t) and to predict the estimated process output in the current sampling run ($\hat{y}_t$) via the first order linear predictive model. Then we define the predictive error $e_t = y_t - \hat{y}_t$ and obtain a weighting predictive value (a_t) by the operation of EWMA filter. Finally, the process parameter of next run will be obtained via comparing a_t and the desired output T.

From the concept of EWMA R2R controller we have mentioned above, equation (3.1) and (3.2) will be used as the models as the real process of CMP equipment. EWMA R2R control rule is calculated as shown in Figure 3.4. The controller is described by the following:

(1) The setup of the real process model:

In order to characterize the drifts and shifts in the removal rate due to pad aging and other factors in real CMP process, two process model, as shown in equation (3.1) and (3.2), are obtained by modifying Preston equation, Luo and Dornfeld equation. They will be used in the simulations.

Preston equation:

$$y_t = K_p \times x_{t-1} \times v + K_E \times \varepsilon - K_D \times n \tag{3.1}$$

where y_t is the removal rate, K_p is the process factor, x_{t-1} is the down force, v is the relative speed between the polishing pad and wafer, K_E is the scaling factor of white noise, ε is the white noise, K_D is the degrading rate, and n is the run number of the process [25][26].

Luo and Dornfeld equation:

$$y_t = C_2[1-\Phi(3-C_1 \times x_{t-1}{}^{1/3})] \times \sqrt{x_{t-1}} \times v + K_E \times \varepsilon - K_D \times n \quad (3.2)$$

where y_t is the removal rate, Φ is the normal cumulative distribution function, x_{t-1} is the down force, v is the relative speed between the polishing pad and wafer, K_E is the scaling factor of white noise, ε is the white noise, K_D is the degrading rate, and n is the run number of the process. C_1 and C_2 is set to be 0.0113 and 30503 in addition according to the experiment in [19].

(2) Predictive model:

$$\hat{y}_t = a_{t-1} + b \times x_{t-1} \quad (3.3)$$

where $\hat{y}_t$ is the estimated process output in the current sampling run, a_{t-1} is the disturbance, b is the gain matrix of the process estimator, x_{t-1} is the down force. The predictive model is established by the method of the linear regression in statistics.

(3) Updating the value of a:

$$e_t = y_t - \hat{y}_t \quad (3.4)$$

where e_t is the difference between the current process output and its estimated value.

$$a_t = \lambda \times e_t + a_{t-1} \quad (3.5)$$

where λ is the weighting factor of the EWMA operator and a reference value for performance evaluation. According to equation (3.5), the predictive model of next run can be obtained as equation (3.6).

$$\hat{y}_{t+1} = a_t + b \times x_t \quad (3.6)$$

where x_t is the process input of next run.

(4) The output of the controller:

The suitable process parameters set to achieve the desired outputs can be calculated by equation (3.7), which is derived from equation (3.6) with $\hat{y}_t$ being replaced by the desired output T.

$$x_t = \frac{T - a_t}{b} \tag{3.7}$$

EWMA R2R controller can be established by the four steps mentioned above and the process control input of each run can be calculated by the same way in order to control the removal rate to research the desired target T. The equation (3.1) and (3.2) will be discussed as the Preston equation, Luo and Dornfeld equation respectively and the simulations results of EWMA R2R control will also be discussed in next chapter [25] [26].

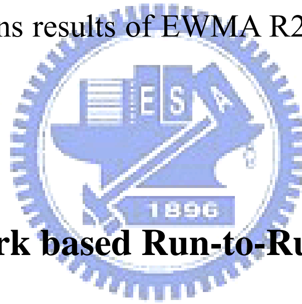

3.4 Fuzzy-Neural Network based Run-to-Run Control System

3.4.1 Radial Basis Function based Fuzzy-Neural Network

In this research, the improved controller based on fuzzy-neural network theory which is mentioned by several articles will be adopted [28] [27] [25] [26]. The conventional fuzzy-neural network consists of six successive layers which are input, fuzzification, rule-base, normalization, defuzzification, and output in sequence as shown in Fig 3.5. Due to computation of complexity and overhead, the six layers are be reduced to four layers proposed by WANG [27]. They are input, fuzzification, rule-base, and output in sequence as shown in Fig 3.6. The calculation of each layer is introduced as follows:

(1) Layer 1 : Input layer

In this research, the input variable is fed to the network which is mentioned in [26] without normalizing.

(2) Layer 2 : Fuzzification layer

The operation of this layer is to transfer the input variable by the membership function to become the grade of the membership, the process is called Fuzzification which is shown in equation (3.8).

$$m_{nj} = \exp[-\beta(\frac{x_n - a_{nj}}{\alpha_{nj}})^2] \quad (3.8)$$

where the maximum value is 1, the minimum value is 0, a_{nj} is the center of the membership function, α_{nj} is the width of the membership function, β is a constant. The curve of the membership function can be adjusted by tuning α_{nj} and β. Because the method of uniform divide is adopted, the range of the membership function is defined by the range of the input variable but not between -1 and 1. For an example, if the range of the input pressure is between 6~9 psi, the range of the membership function can be definded in 6~9 psi, shown in Fig 3.7. The method of uniform division is executed as the following:

$$c = \frac{H - L}{m - 1} \quad (3.9)$$

where c is the interval, H is the high limit of the input variable, L is the lower limit of the input variable, m is the divided number of the membership function. For an example, if the divided numbers of the membership function is decided to be 5 $(m = 5)$ in 6~9 psi, the middle

values of the membership function will be 6, 6.75, 7.5, 8.25 and 9 respectively.

(3) Layer 3 : Rule-base layer

Each neuron at this layer represents a fuzzy rule and executes "T-norm" operation, or "intersection" as shown in equation (3.10).

$$z_1 = m_{11} \cap m_{21}, \quad z_2 = m_{11} \cap m_{22}, \cdots \tag{3.10}$$

(4) Layer 4 : Output layer

At this layer, the products of the output of neuron and the weighting will be all summed up to derive to the output value of the output layer. It is shown as follow:

$$y_k = \sum_{i=1}^{l} z_i \times w_{ki} \qquad k = 1, \cdots, K \tag{3.11}$$

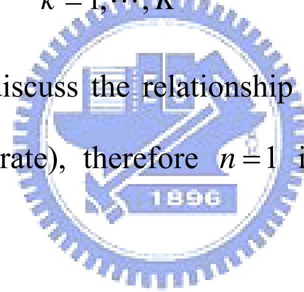

In this thesis, we only discuss the relationship between single input (pressure) and single output (removal rate), therefore $n = 1$ in equation (3.8) and $k = 1$ in equation (3.11).

3.4.2 The Training of the Network

The characteristic of this network is that the training approach has been divided into rough-tune and fine-tune. While rough-tune means that the goal of training can be achieved by changing the weighting between rule-base layer and output layer rapidly, fine-tune means that the training error can be reduced by tuning the width of the membership function.

(1) Rough-tune

The rough-tune can be divided into batch and increment.

(a) Batch

If the weighting number is N and the training pattern is P, the equation (3.11) can be represented in the form of matrix as follow:

$$\begin{bmatrix} z_{11} & z_{21} & \cdots & z_{N1} \\ z_{12} & z_{22} & \cdots & z_{N2} \\ z_{13} & z_{23} & \cdots & z_{N3} \\ \vdots & \vdots & \vdots & \vdots \\ z_{1P} & z_{2P} & \cdots & z_{NP} \end{bmatrix} \begin{bmatrix} w_1 \\ w_2 \\ w_3 \\ \vdots \\ w_N \end{bmatrix} = \begin{bmatrix} y_{d1} \\ y_{d2} \\ y_{d3} \\ \vdots \\ y_{dP} \end{bmatrix}$$

$$\Rightarrow ZW = Y \tag{3.12}$$

when P > N, the number of equation is larger than the number of unknown. It is no exact solution. The least squares method is used as follow:

$$W = (Z^T Z)^{-1} Z^T Y \tag{3.13}$$

when P ≤ N, the number of equation is samll than the number of unknown. There are infinite solutions. Minimum norm solution is determined as below:

$$W = Z^T (ZZ^T)^{-1} Y \tag{3.14}$$

If the training patterns are superfluous, the network will be closer to the real situation. However, the training errors increase as the training patterns increase. If the training patterns are insufficient, the network can not represent the real situation. It should alert user's attention when the insufficient training occurs.

(b) Increment

The Increment method uses the concept of error back propagation to tune the weighting between layer 3 and layer 4 as shown below:

$$\Delta w_i = -\eta \frac{\partial E}{\partial w_i} \tag{3.15}$$

where $E = \frac{1}{2}(y_d - y)^2$ is the error term, η is the parameter of training. According to the chain-rule

$$\frac{\partial E}{\partial w_i} = \frac{\partial E}{\partial y}\frac{\partial y}{\partial w_i} = -(y_d - y)z_i \tag{3.16}$$

Therefore equation (3.15) becomes

$$\Delta w_i = \eta(y_d - y)z_i \tag{3.17}$$

Finally the updating rule of the weighting can be represented as

$$w_i^{'} = w_i + \Delta w_i \tag{3.18}$$

(2) Fine-tune

The fine-tune method is tuning the width of the member function corresponds the output value z_i in the layer 3.

$$z_i = \exp\left[-\beta\left(\frac{x-a_i}{\alpha_i}\right)^2\right] \tag{3.19}$$

It also uses the concept of error back propagation to tune the width of the membership function.

$$\Delta\alpha_i = -\eta\frac{\partial E}{\partial \alpha_i} \tag{3.20}$$

By the chain-rule

$$\frac{\partial E}{\partial \alpha_i} = -(y_d - y)w_i \times \exp[-\beta(\frac{x-a_i}{\alpha_i})^2][2\beta(x-a_i)^2\alpha_i^{-3}] \tag{3.21}$$

Therefore the variation of α can be represented as

$$\Delta\alpha_i = \eta(y_d - y)w_i \times \exp[-\beta(\frac{x-a_i}{\alpha_i})^2][2\beta(x-a_i)^2\alpha_i^{-3}] \tag{3.22}$$

Finally the updating rule of α can be written as

$$\alpha_i^{'} = \alpha_i + \Delta\alpha_i \tag{3.23}$$

The training method in this research adopts the least square method of rough-tune and also fine-tune to reduce the error. It then proceeds to control the process models, aiming at Preston equation and Luo and Dornfeld equation respectively to find the optimal parameters of the process [26] [27].

3.4.3 The Concept of Zero Error Tracking Control

To consider the training speed of the network and to make the tracking error of the system to research zero for a specific time, the zero error tracking control is used as shown in equation (3.24). The concept is expected that the error of next run can be smaller than this run to correct the control input. The mathematical calculation can be found in [26].

$$e_t^E = \gamma \cdot e_{t-1} \tag{3.24}$$

where $0 < \gamma < 1$. That is when $t \to \infty$ as $e \to 0$.

The inference about proceeding the correction of the controller aimed at Preston equation can be find in [26]. The same method which is used aimed at Luo and Dornfeld equation is described as follows:

First the desired output is assumed as T, the process output of last run and error is y_{t-1} and e_{t-1} respectively. Hence, the equation can be represented as below:

$$e_{t-1} = T - y_{t-1} \tag{3.25}$$

And the excepted error of this run can be obtained by the same way as follow:

$$e_t^E = T - y_t \tag{3.26}$$

The Luo and Dornfeld equation (Eq. 3.2) is used as the process model in the simulation, where the input x_{t-1} is replaced by P (Down Force), other parameters are set to be constant, then is substituted into equation (3.26).

$$e_t = T - \{30503[1 - \Phi(3 - 0.0113 x_{t-1}{}^{1/3})]\sqrt{x_{t-1}} V + K_E \times \varepsilon - K_d \times n\} \tag{3.27}$$

Further equation (3.25) and equation (3.27) are substituted into equation (3.24),

$$T - \{30503[1 - \Phi(3 - 0.0113 x_{t-1}^{E}{}^{1/3})]\sqrt{x_{t-1}^E} V + K_E \times \varepsilon - K_D \times n\} = \gamma (T - y_{t-1}) \tag{3.28}$$

where x_{t-1}^E is represented as the expected input value of this run in order to arrive at

the desired value. Then the equation (3.27) and (3.28) can be expressed as below respectively.

$$\frac{T-e_t-(K_E\times\varepsilon-K_D\times n)}{30503V}=\sqrt{x_{t-1}}[1-\Phi(3-0.0113{x_{t-1}}^{1/3})] \tag{3.29}$$

$$\frac{T-\gamma e_{t-1}-(K_E\times\varepsilon-K_D\times n)}{30503V}=\sqrt{x_{t-1}^E}[1-\Phi(3-0.0113{x_{t-1}^E}^{1/3})] \tag{3.30}$$

Form equation (3.29) and (3.30), it is obvious that the input value is included in the cumulative distribution function. If the control input is limited to 5~8 psi, the average of $\Phi(3-0.0113{x_{t-1}}^{1/3})$ is 0.9986. Hence the average of $[1-\Phi(3-0.0113{x_{t-1}}^{1/3}]$ is 0.0014. Therefore $[1-\Phi(3-0.0113{x_{t-1}}^{1/3}]$ and $[1-\Phi(3-0.0113{x_{t-1}^E}^{1/3}]$ can be taken as the same constant and divided to the left side of the equation, after that the equations can be arranged as equation (3.31) and (3.32).

$$x_{t-1}=\frac{[T-e_t-(K_E\times\varepsilon-K_D\times n)]^2}{CV^2} \tag{3.31}$$

$$x_{t-1}^E=\frac{[T-\gamma e_{t-1}-(K_E\times\varepsilon-K_D\times n)]^2}{CV^2} \tag{3.32}$$

The correction of process input can be obtained via subtract (3.31) from (3.32) as shown below:

$$\Delta x_{t-1}=x_{t-1}^E-x_{t-1}=\frac{\gamma^2{e_{t-1}}^2-{e_t}^2+2(e_t-\gamma e_{t-1})(T-K_E\times\varepsilon+K_D\times n)}{CV^2} \tag{3.33}$$

Because of desiring to eliminate the error, we assume $x_{t-1}^E=x_t$. Finally the next run of process control input can be obtained as follow:

$$x_t=x_{t-1}+\Delta x_{t-1} \tag{3.34}$$

From above, when the process model is Luo and Dornfeld equation, the controller will control the process input to reach at the desired value by equation (3.34).

However the denominator term of equation (3.33) in actual system is not easy to compute in real world [26]. Therefore the equation (3.2) can be used as the process model in the same way, where the input value is P (Down Force), other parameters

are constant, then proceeds to calculate partial differentiation with respect to input x_{t-1} as shown below.

$$\frac{\partial y}{\partial x_{t-1}} = [1-\frac{1}{\sqrt{2\pi}}\int_{-\infty}^{3-0.0113{x_{t-1}}^{1/3}} e^{-(1/2)t^2}dt]'[30503V{x_{t-1}}^{1/2}]$$

$$+[1-\frac{1}{\sqrt{2\pi}}\int_{-\infty}^{3-0.0113{x_{t-1}}^{1/3}} e^{-(1/2)t^2}dt][0.5\times 30503V{x_{t-1}}^{-(1/2)}] \qquad (3.35)$$

where the control input is to be 5~8 psi that substitute into $\frac{1}{\sqrt{2\pi}}\int_{-\infty}^{3-0.0113{x_{t-1}}^{1/3}} e^{-(1/2)t^2}dt$, then $\frac{1}{\sqrt{2\pi}}\int_{-\infty}^{3-0.0113{x_{t-1}}^{1/3}} e^{-(1/2)t^2}dt = 0.3948-2.1\times 10^{-6}x_{t-1}$ can be obtained by linear regression. Therefore equation (3.35) can be expressed as follow:

$$\frac{\partial y}{\partial x_{t-1}} = [1-(0.3984-2.1\times 10^{-6}x_{t-1})]'[30503V{x_{t-1}}^{1/2}]$$

$$+[1-(0.3984-2.1\times 10^{-6}x_{t-1})][0.5\times 30503V{x_{t-1}}^{-(1/2)}]$$

$$=30503V[3.15\times 10^{-6}{x_{t-1}}^{1/2}+0.3008{x_{t-1}}^{-(1/2)}] \qquad (3.36)$$

It is difficult to obtain the relationship of partial differentiation between input and output. In the thesis, the concept of fuzzy-neural network is used to derive the relationship of partial differentiation between input and output to be the predicted input value of system. According to the chain-rule:

$$\frac{\partial y}{\partial x} = \frac{\partial y}{\partial z_i}\frac{\partial z_i}{\partial x} \qquad (3.37)$$

The output of network can be represented as below:

$$y = \sum_{i=1}^{k} w_i z_i \qquad (3.38)$$

Then to proceed partial differentiation aim at y.

$$\frac{\partial y}{\partial z_i} = w_i \qquad (3.39)$$

Because of the single input, z value is the corresponding membership function:

$$z_i = \exp[-\beta(\frac{x-a_i}{\alpha_i})^2] \qquad (3.40)$$

Then to proceed partial differentiation aim at z_i.

$$\frac{\partial z_i}{\partial x} = \exp[-\beta(\frac{x-a_i}{\alpha_i})^2][-2\beta\alpha_i^{-2}(x-a_i)] \tag{3.41}$$

Finally the relationship of partial differentiation between input and output can be obtained by substituting equations (3.39) and (3.41) into equation (3.37) as shown below:

$$\frac{\partial y}{\partial x} = \sum_{i=1}^{k}\{w_i \times \exp[-\beta(\frac{x-a_i}{\alpha_i})^2][-2\beta\alpha_i^{-2}(x-a_i)]\} \tag{3.42}$$

In the thesis, the equation (3.42) will be utilized to calculate the relationship of partial differentiation between input and output.

Design a suitable controller of CMP equipment to control the simulator is the key objective of this thesis. At the same time, the simulator proceeds to simulate the variation of removal rate, feedbacks the result to the controller after computation, finds the optimal process parameters iteratively. Combining to the theory mentioned above and the strategy of run-to-run control, a run-to-run FNN controller is developed as shown as fig 3.8. The controller provides the training data to fuzzy-neural network (FNN) predictor, and then utilizes equation (3.42) to calculate the relationship of partial differentiation between input and output, feeds the controller via a gain K finally. It proceeds to control process output by adjusting the gain K continuously [26]. Furthermore, it focuses on the process, and sets e_{t-1} to be zero and input to be x_{t-1}, then obtains the process output y_t via the process model, compares the output with the desired value (target T) to obtain error e_t, finally calculates the control input of next run by the controller. It corrects the control input iteratively by the controller until the process output reaches the desired target.

Chapter 4

Simulation and Analysis for CMP Controller

The EWMA controller and zero error tracking fuzzy neural network (FNN) controller will be used for Preston equation and Luo and Dornfeld equation respectively to conduct control simulation and analysis in this chapter.

4.1 Simulations using Preston Equation for S_iO_2 CMP Process

First, the process parameters in Preston equation (3.1) will be set as follow: where p = 6 psi, v = 50, ε = white noise, N~(0,1), mean=0, variance=1, n = 200, K_p = 7.5, K_E = 83.25, K_D = 3.8.

Next, the EWMA controller and zero error tracking fuzzy neural network controller will be used for Preston equation to conduct control simulation and analysis.

4.1.1 EWMA controller for Preston Equation

For EWMA controller, the weighting value λ is chosen to be 0.8 at no conditioning situation and the variation of removal rate from wafer to wafer for S_iO_2 CMP process is depicted in Fig 4.1. The objective is to control the removal rate at 2200 ($\mathring{A}$/min). The predictive model of EWMA controller, the equation is $y = 343.7898 + 316.9260x$ when the range of pressure input be limited at 5~8 psi, is depicted in Fig 4.2. The solid line represents the relative trajectory between input and

output of process model (Preston equation), the dotted line represents the predictive trajectory of EWMA controller, and SSE (Sum Square Error) between the two trajectories is equal to 1.9241e+5 $(\overset{\circ}{A}/\min)^2$.

The control result via EWMA R2R controller is shown in Fig 4.3, where the solid line denotes the result without control, the dotted line denotes the desired value of process, the circled ones denotes the result with EWMA controller. It can been seen that the process target can be controlled at 2200 ($\overset{\circ}{A}$/min) by EWMA controller and MSE (Mean Square Error) is equal to 1.4693e+4 $(\overset{\circ}{A}/\min)^2$, then the variation of control input trajectory is shown in Fig 4.4. When the process proceeds, the prediction of EWMA predictor also changes from wafer to wafer, and the predictive error of each wafer run is shown in Fig 4.5, and SSE is equal to 6.0728e+3 $(\overset{\circ}{A}/\min)^2$. From the data above, EWMA R2R controller can control the process output at the desired value, but it is obvious that the first order linear predictor can not simulate the nonlinear process model from the predictive error in Fig 4.2.

4.1.2 Zero Error Tracking Fuzzy-Neural Network Controller for Preston Equation

In the zero error tracking fuzzy neural network controller, the numbers of fine-tune (epoch) is set to be 6000, the training parameter η is chosen to 1.0e-9, the α 、β of membership function is set to 1.6 and 4 respectively, the γ of error tracking is set to 0.5 and the gain K is set to 1. The variation of removal rate changes from wafer to wafer increased under no control is depicted in Fig 4.1. The object is to control the removal rate at 2200 ($\overset{\circ}{A}$/min). The predictive result of FNN

Predictor when the range of pressure input be limited at 5~8 psi is illustrated in Fig 4.6, and the solid line represents the relative trajectory between input and output of process model (Preston equation), the dotted line represents the predictive trajectory of FNN Predictor, and SSE is equal to 3.6249e+4 $(\mathring{A}/\min)^2$ which is less than EWMA Predictor (1.9241e+5 $(\mathring{A}/\min)^2$). Further, SSE converges to 3.6220e+4 $(\mathring{A}/\min)^2$ after fine-tune which is shown in Fig 4.7. Therefore, it is known that the fine-tuned one can reduce SSE truly but the performance is limited, the result can be found in Fig 4.8.

The control result via zero error tracking fuzzy neural network controller is shown in Fig 4.9, where the solid line denotes the result without controlling, the dotted line denotes the desired value of process, the circled ones denotes the result with controlling. It can been seen that the process target can be controlled at 2200 $(\mathring{A}/\min)$ by the controller and MSE (Mean Square Error) is equal to 8.5957e+3 $(\mathring{A}/\min)^2$ which is less than EWMA controller (1.4693e+4 $(\mathring{A}/\min)^2$), then the variation of control input trajectory is shown in Fig 4.10.

4.1.3 The Comparisons of Simulation Results

From the simulation results above, the predictive ability and the control result of zero error tracking fuzzy neural network controller using Preston equation are both better than EWMA controller, but the algorithm and tuning parameters are more complex than EWMA, the computation burden is higher for zero error tracking fuzzy neural network controller.

4.2 Simulations using Luo and Dornfeld Equation for Copper CMP Process

First, the process parameters for Luo and Dornfeld equation (3.2) will be set as follow: where $C_1 = 30503$; $C_2 = 0.0113$; $p = 6$ psi, $v = 40$, $\varepsilon =$ white noise, N~(0,1), mean=0, variance=1, $n = 200$, $K_E = 215.75$, $K_D = 5$

Next, the EWMA controller and zero error tracking fuzzy neural network controller will be used for Luo and Dornfeld equation to conduct the control simulation and analysis.

4.2.1 EWMA Controller for Luo and Dornfeld Equation

For EWMA controller, the weighting value λ is chosen to be 0.8 at no conditioning situation and the variation of removal rate from wafer to wafer for CMP process is depicted in Fig 4.11. The objective is to control the removal rate at 4300 ($\mathring{A}$/min). The predictive model of EWMA controller, the equation is $y = 2418.2 + 317.31x$ when the range of pressure input be limited at 5~8 psi is illustrated in Fig 4.12, and the solid line represents the relative trajectory between input and output of process model (Luo and Dornfeld equation), the dotted line represents the predictive trajectory of EWMA controller, and SSE between the two trajectories is equal to 2.7205e+5 $(\mathring{A}/\min)^2$.

The control result via EWMA R2R controller is shown in Fig 4.13, where the solid line denotes the result without control, the dotted line denotes the desired value of process, the circled ones denotes the result with EWMA controller. It can been seen that the process target can be controlled at 4300 ($\mathring{A}$/min) by EWMA controller

and MSE is equal to 7.2469e+4 $(\mathring{A}/\min)^2$, then the variation of control input trajectory is shown in Fig 4.14. When the process proceeds, the prediction of EWMA predictor also changes from wafer to wafer, and the predictive error of each wafer run is shown in Fig 4.15, and SSE is equal to 4.6574e+4 $(\mathring{A}/\min)^2$. From above, it is known that EWMA R2R controller can control the process output at the desired value, but it is obvious that the first order linear predictor can not simulate the nonlinear process model from the predictive error in Fig 4.12.

4.2.2 Zero Error Tracking Fuzzy-Neural Network Controller for Luo and Dornfeld Equation

In the zero error tracking fuzzy neural network controller, the numbers of fine-tune (epoch) is set to be 6000, the training parameter η is chosen to be 1.0e-9, the α、β of membership function is set to be 1.6 and 4 respectively, the γ of error tracking is set to 0.5 and the gain K is set to 2. The variation of removal rate changes from wafer to wafer under no control is depicted in Fig 4.11. The objective is to control the removal rate at 4300 ($\mathring{A}$/min). The predictive result of FNN Predictor when the range of pressure input be limited at 5~8 psi is illustrated in Fig 4.16, and the solid line represents the relative trajectory between input and output of process model (Luo and Dornfeld equation), the dotted line represents the predictive trajectory of FNN Predictor, and SSE is equal to 3.4110e+4 $(\mathring{A}/\min)^2$ which is less than EWMA Predictor (2.7205e+5 $(\mathring{A}/\min)^2$). Further, SSE converges to 3.3848e+4 $(\mathring{A}/\min)^2$ after fine-tune which is shown in Fig 4.17. Therefore, it is known that the fine-tuned one can reduce SSE truly but the performance is limited,

the result can be found in Fig 4.18.

The control result via zero error tracking fuzzy neural network controller is shown in Fig 4.19, where the solid line denotes the result without controlling, the dotted line denotes the desired value of process, the circled ones denotes the result with controlling. It can been seen that the process target can be controlled at 4300 ($\overset{\circ}{A}$/min) by the controller and MSE (Mean Square Error) is equal to 5.9173e+4 $(\overset{\circ}{A}/min)^2$ which is less than EWMA controller (7.2469e+4) $(\overset{\circ}{A}/min)^2$, then the variation of control input trajectory is shown in Fig 4.20.

4.2.3 The Comparisons of Simulation Results

From the simulation results above, the predictive ability and the control result of zero error tracking fuzzy neural network controller using Luo and Dornfeld equation are both better than EWMA controller, but the algorithm and tuning parameters are more complex than EWMA, the computation burden is higher than zero error tracking fuzzy neural network controller.

4.3 Summary of Simulations

In the above simulations, it is obvious that the zero error tracking fuzzy neural network controller can control both S_iO_2 CMP and Copper CMP process via tuning of gain constant K, and the predictive ability and control results are all better than EWMA controller. Next chapter, all of the controllers and plants will be included in the Operator Process Interface (OPI) to provide a reference for the operator who operates the CMP equipment.

Chapter 5

Run-To-Run Controller Implementation

In this chapter, the R2R control solution will be presented. The purpose is to develop an OPI module to provide a user interface platform for viewing the operation of the system. The control system utilizes model-base control techniques and control algorithm of EWMA and FNN to derive recipe improvements, and determines better recipe parameters for the next process cycle.

5.1 Hardware and Module Descriptions

After completing simulations of controllers and plants, the control algorithms and the plants will be implemented into different industrial computers individually to develop the OPI module. The industrial computer is a specialized hardware reserved for CMP equipment engineers, and designed for data collection, the OPI module available by the equipment side for operators too. It is called Equipment and Engineering System (EES) BOX by Industrial Technology Research Institute (ITRI) as shown in Fig 5.1. The EES BOX uses the Industrial PC (IPC) motherboard, and provides built-in and/or extended capabilities for sensor integration, data acquisition period less than 1 sec, and patented SECS protection mechanism for pass-through configuration, and uses stainless steel case to meet the clean room requirement in wafer FAB. The detailed specifications are shown as Table 5.1 [22] [29].

Between two independent computers, an RS-232 hardware is used to build the communication module to simulate the signal transmission between the real world machines as shown in Fig. 5.2. The controller sends the initial control message to

the simulator via RS-232 module, then the simulator uses a timer component to receive the data from controller continuously and simulates the state variables and interactive behavior of CMP equipment via mathematical model, and transfers the result to output information to the controller. Through R2R control capability, the optimal recipe for CMP equipment will be obtained to achieve the control target simultaneously. In other words, by inputting parameters to the system, the user can forecast a new recipe in the set-up run of the process and can do research and analysis according to the data of each wafer run. It is called Simulation Run mode. In addition, we design a R2R Control mode on the controller side for the user to obtain a new recipe and predict CMP removal rate in the next processing run using the removal rate of real CMP process data. It can be used as recommendation from R2R controller for user to control the CMP process.

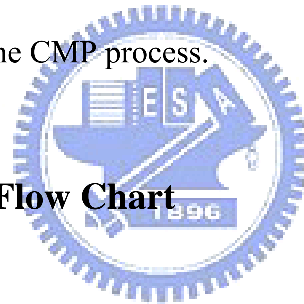

5.2 Computer Program Flow Chart

Direct hardware access in 32-bit Windows is generally not allowed. In doing Serial and COM port communication, we use the Win32 API CreateFile and the Win32 communication functions in BC++ Builder. It needs to handle communication resource (such as getting hold of COM1), and sets the property of dwCreationDistribution to OPEN_EXISTING, and further, the value of hTemplate must be NULL, then the Serial and COM port communication can be opened by using the Win32 API CreateFile.

In the Simulation Run Mode, we implement the Timer of VCL component both in the simulator PC and controller PC respectively and then write the main program in them, and set the interval to 500 milliseconds. The purpose is to poll the buffer to check if there is data obtained by the Timer component continuously. We utility this

structure to reach the R2R control goal. The main program in the control system is presented in Fig 5.3 that we use Readfile to receive data which is in the buffer, and set a counter to keep track the wafer run which is set up by the user. Afterward, the program accesses the Control Rule block to run the rule selected by the user, where we use "if and else if" rule to design the Control Rule block. After that, the program will run the Mean Square Error (MSE) and show the data at the OPI, and then send the result to the output buffer by the Writefile. Finally, the decision block will check whether the counter is smaller than the value of the wafer run or not. If the result is "yes", the program will return to Readfile and run the sequence again. If the result is "no", the program will terminate the Timer component and stop receiving data. The main program of the Timer component in the simulator is shown in Fig 5.4. Similarly, Readfile will receive the data from the buffer and check whether the buffer is empty or not. If there is the character in the buffer, the program will access next decision block to check what the character is. If the character is the control character, the command will be executed according to meaning of the control character and then go back to Readfile to receive data again. If it is not the control character, the receiving data will access "plant" block and run the "plant" selected by user to process it. If there is no control character and receiving data in the buffer, the program will return to Readfile till the control character is in the buffer again. We implement many control characters in the Timer component for controlling the simulator side, and the Timer component will not be terminated unless the window of the simulator is closed. The design concept is that the controller can control simulator automatically depending on the different initial setting. By this way, we do not need to setup two computers respectively, but the simulator still can be controlled by the controller. The main concern about designing the simulator and controller is that we want to expand the algorithm in Control Rule block and add the

new equations in “plant” block of the system easily in the future.

In the R2R Control mode, the main computer program flow chart of the control system is presented as Fig 5.5. The input parameters will be fed into the condition block to choose the algorithm and plant selected by the user, where the Rule1, Rule2, Plant1 and Plant2 represent EWMA control law, FNN control law, Preston equation and Luo and Dornfeld equation respectively. After executing the control algorithm, the program will compute the optimal pressure and predictive removal rate in the next run to provide the data for the CMP process user. The program will run the same procedure after inputting the next command.

In the trend plot part, we use the TChart component to present each plot on the OPI and the data obtained from the Timer component. In the data storage part, we create a new Form and use the StringGrid component on it to show the data that we want to store, and use the SaveDialog component to save the data as a text file. The schematic procedures of the OPI and the operational procedures will be introduced in next section.

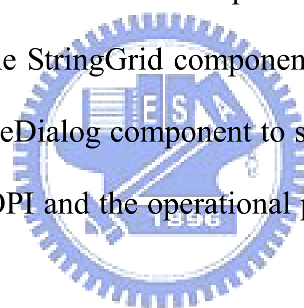

5.3 Introduction of Run-To-Run Operator Process Interface

The OPI of the controller developed by BC++ Builder is shown in Fig 5.6, and the OPI of the simulator which is also design by BC++ Builder is shown in Fig 5.7. Before entering the communication module of OPI environment, the user must press “open” button first, then key in the user name and password to open the COM port of RS-232 module as shown in Fig 5.8. There are two modes in the OPI environment that the users can select the one which meets their requirements. The functions and operational procedures are described as follow.

In the Simulation Run mode, the user can choose different control rules to

control different plants via the “Initial Setting” section to see the different results, then key in the numbers of wafer run and the initial input pressure. Further the simulator will display the same condition as the controller for the purpose of controlling simulator by the controller. When all the initial settings are set up completely, the program will be executed by pressing the “Execute” button as shown in Fig 5.9. After the progress bar being filled with blue color, it means that the simulation process has finished, and the result will be displayed in the “Result” section as shown in Fig 5.10. It includes Mean Square Error (MSE) and the optimal control input, and the simulator will display the same result as shown in Fig 5.11. Furthermore, the R2R plots of down force, controlled plant output and uncontrolled plant output can be displayed by pressing the “Pressure”, “Control” and “Uncontrol” buttons respectively as shown in Fig 5.12. Finally, simulation data can be exported to a data file by pressing the “Export” button. OPI pops up a frame with the result data as shown in Fig 5.13. The data can be saved as a text file by pressing the “Save As” button.

In the R2R Control Mode, the user can input the metrology data which is obtained by the actual CMP process to get the optimal input pressure and predict the removal rate. If the user presses the “Execute” button twice, the program will be executed two times. At the same time, the blank space of wafer run will display 2 and the removal rate of next run, and so on as shown in Fig 5.14. Therefore, the user can refer to the information to adjust his recipe to reach the goal of removal rate in R2R manner. In the same way, the plots of down force, controlled plant output and uncontrolled plant output, can be displayed by pressing the “Pressure”, “Control” and “Uncontrol” buttons respectively as shown in Fig 5.15. The data can be exported to a data file by pressing the “Export” button. OPI can pop up the result data as shown in Fig 5.13. The data can also be saved as a text file by pressing the “Save As” button. The standard operation procedures (SOP) have been illustrated as above that a user

can operate the simulator and obtain the process information when needed.

5.4 Summary and Contribution

The R2R component of the control solution described above can be applied to control remaining thickness of S_iO_2 film and Copper film by CMP process. We can compare the process with and without R2R control as in Fig 5.12. Specifically, the software shows that

(1) the controller provides the correct recipe for down force as the removal rate decreasing from wafer to wafer.

(2) the controller compensates for process drift and keeps the removal rate at target.

(3) the MSE index is used to quantify the mean square error of removal rate and capability of the controller.

According to the information, the engineer and operator can predict the result of CMP processing under controlled or uncontrolled situation, and obtain the recommended input (down force) to reach at the desired removal rate target.

In the system, it can provide a lot of information for the engineers to improve the CMP process. We can highlight four contributions as follows:

(1) CMP process simulator for process simulation:

The simulator and control system can be used as reference resources of CMP processing. According to the result of the simulation, the engineers can adjust the control input to meet the removal rate target wafer to wafer. It also provides the R2R plots of Down Force, controlled plant output and uncontrolled plant output, and the text file of process data of each wafer run as the reference data for engineers are doing research and analysis.

(2) CMP supervisory system for recipe management:

The simulator and control system can be used as supervisory system for recipe management. The user can input different recipe parameter value to obtain different plant outputs and trend charts of down force and removal rate from the supervisory system. By the R2R control framework, the process engineer can obtain the optimal recipe and manage the recipe from wafer to wafer.

(3) CMP process training for operator training:

The simulator and control system can be used as the CMP process training system for operator training. The user can change the configuration of the user interface to realize the relationship between input (down force) and output (removal rate) of CMP equipment.

(4) CMP predictive maintenance system for pad replacement by monitoring of removal rate:

Because the pad will be worn gradually, the removal rate will decrease with time. The process engineer can do pad condition by a diamond disc to reduce the aging of the pad or replace the pad according to monitoring of removal rate shown on the plots. Hence, the process engineer can predict the removal rate and the timing of maintenance for CMP equipment.

Chapter 6

Conclusion and Future Work

Major efforts are underway to move semiconductor manufacturing to fab-wide solutions for advanced process control after initial deployment. However, in the process control, it begins from single equipment and single process initially, then expands to nearby process equipments. Through integrated advanced process control constantly, standard R2R control solutions use feed-forward and feedback data to compensate process drifts and variations and control process output, such as CMP film thickness, to specified targets. A control strategy must be developed that supports control and optimization for fab-wide goals such as overall fab yield and throughput rates through the coordinated control of individual process parameters.

In this thesis, EWMA control law and Fuzzy Neural Network control law are applied to SiO_2 and Copper of CMP process respectively. From the simulation results of chapter 4, it has been proven that Fuzzy Neural Network controller has better control ability than EWMA controller for both SiO_2 and Copper CMP processes. In addition, OPIs of simulator and control system for CMP process have been developed. OPI provides a simulation tool for process engineer to manage and analyze the CMP process. Process engineers can improve CMP processing according to recommendation of simulator and controller wafer to wafer.

Therefore, the following suggestions are addressed to realize FAB wide APC solutions.

1. It allows for complementary utilization of process control and optimization methods for R2R control. The R2R controller can have different optimizations or control algorithms to enhance the robustness of the controller. In order to achieve the goals, the different control rule can be

integrated in the R2R controller, an optimal recipe will be obtained from comparing the weighted advice of the selected algorithm and will be the main output of the R2R control.

2. It requires integration of the Real Time Monitor System (RTMS) designed by ITRI to collect process data and makes a model for the real equipment in the future. Furthermore, it needs to develop a complete controller which uses the concept of feedback loop, and it is expected to control the equipment and to achieve the run-to-run control goal after removing the simulator and connecting the real world equipment.
3. It includes the fault detection and classification (FDC) system to determine if the tool is in an acceptable region where control should be applied, and further serves as front end to filter data to the controllers.

It is expected that this controller architecture can be developed as a data mining tool which is compatible with existing standards and trends in semiconductor manufacturing. It can be easily enhanced to support future process control requirements in wafer FAB.

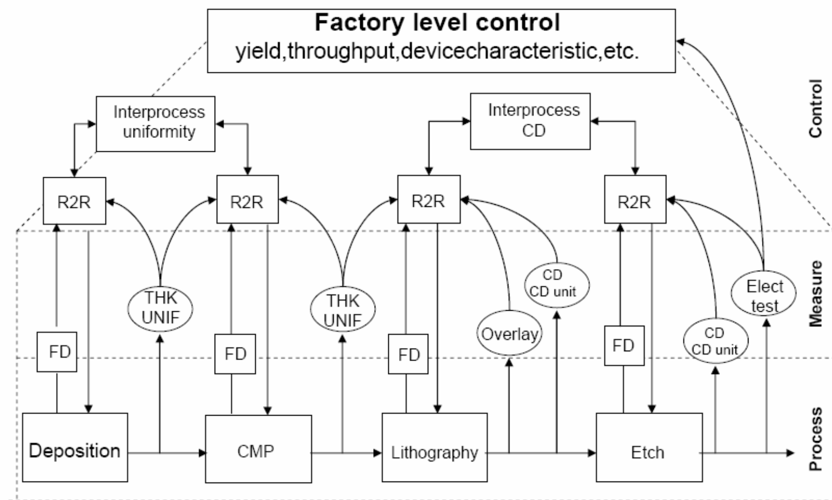

Figure 1.1 Hierarchical control structure [2]

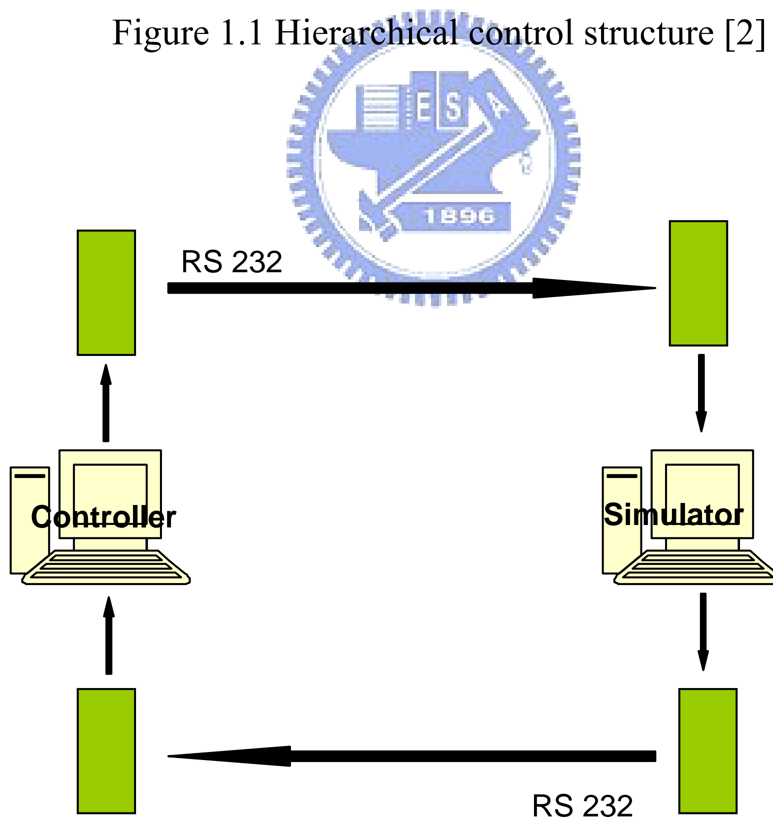

Figure 1.2 The control structure for CMP equipment

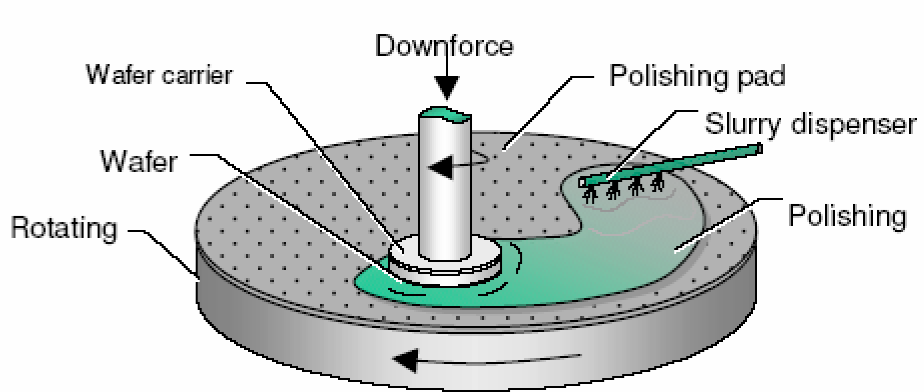

Figure 2.1 The mimic schematic of CMP equipment [9]

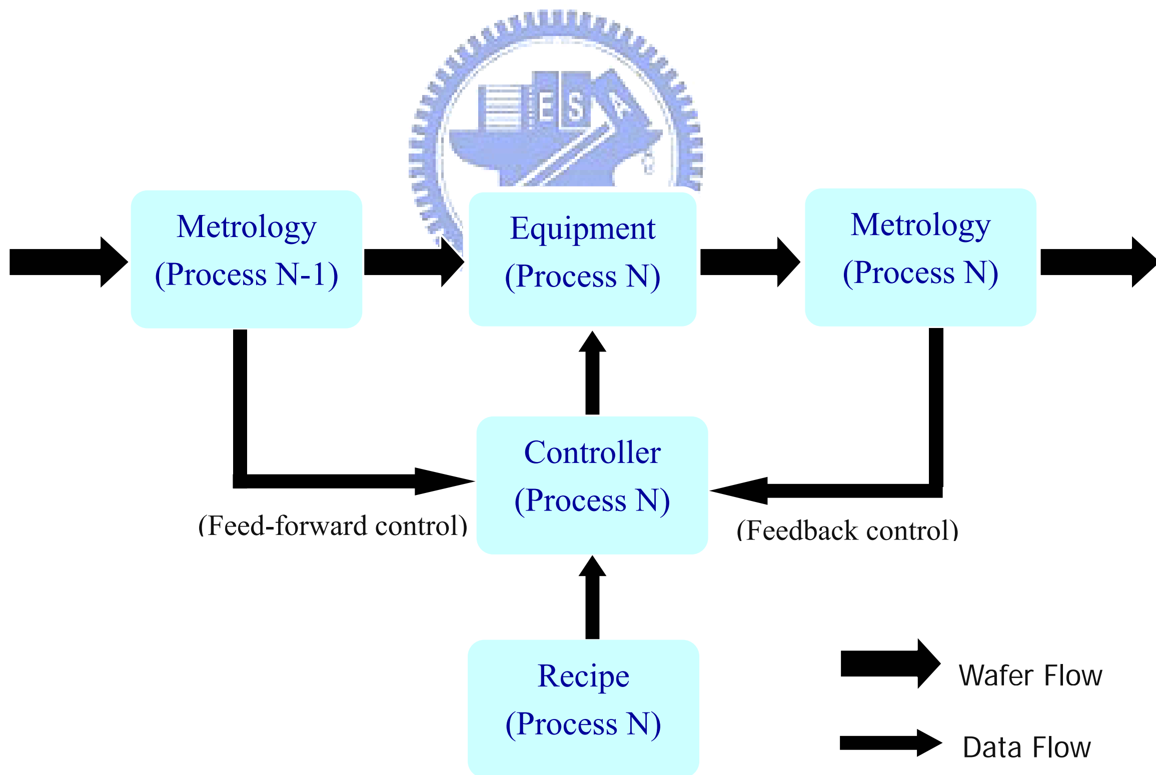

Figure 3.1 R2R control diagram [22]

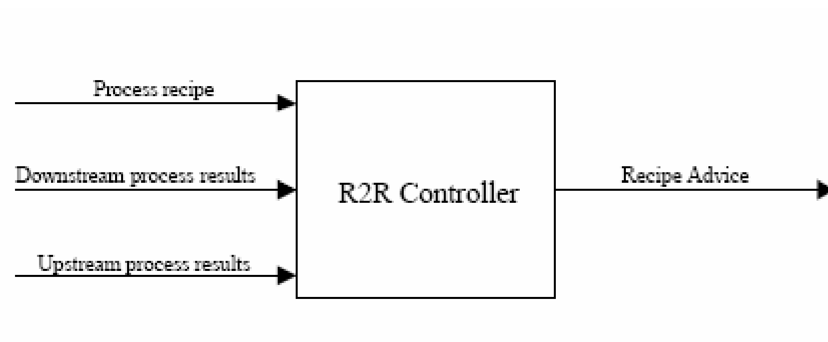

Figure 3.2 The relationship between input and output of R2R controller [22]

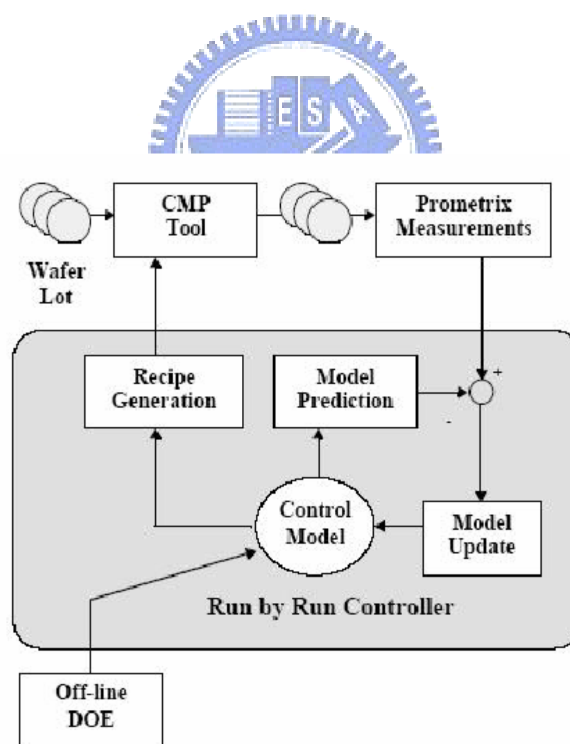

Figure 3.3 CMP R2R process control strategy [13]

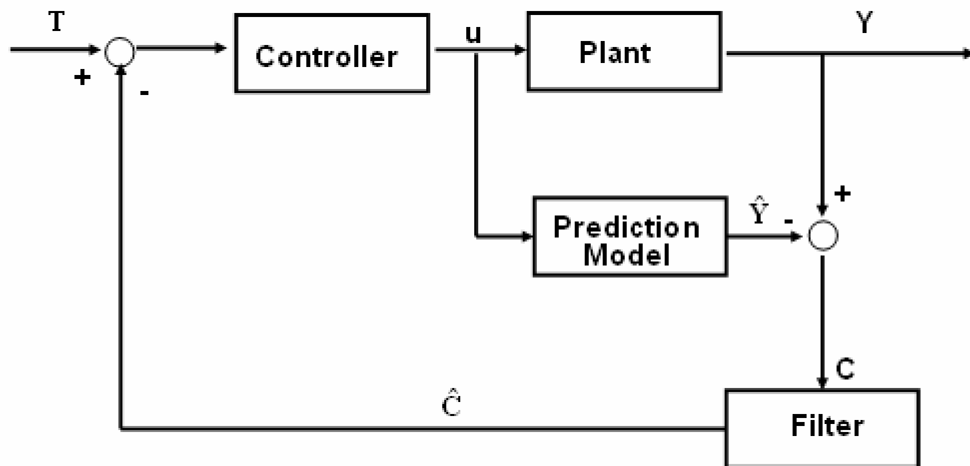

Figure 3.4 EWMA R2R control block diagram

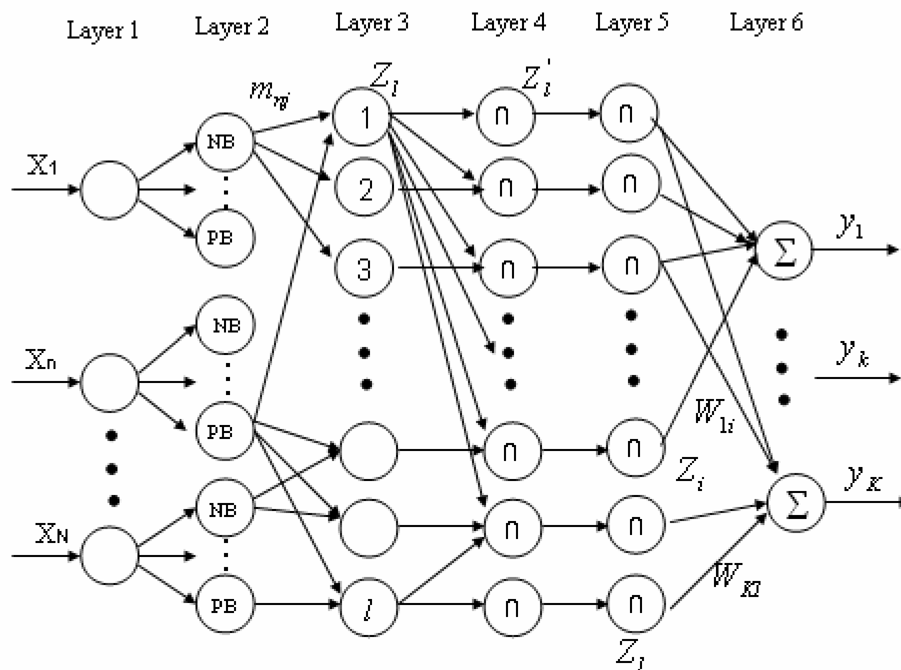

Figure 3.5 Fuzzy Neural Network (FNN) structure

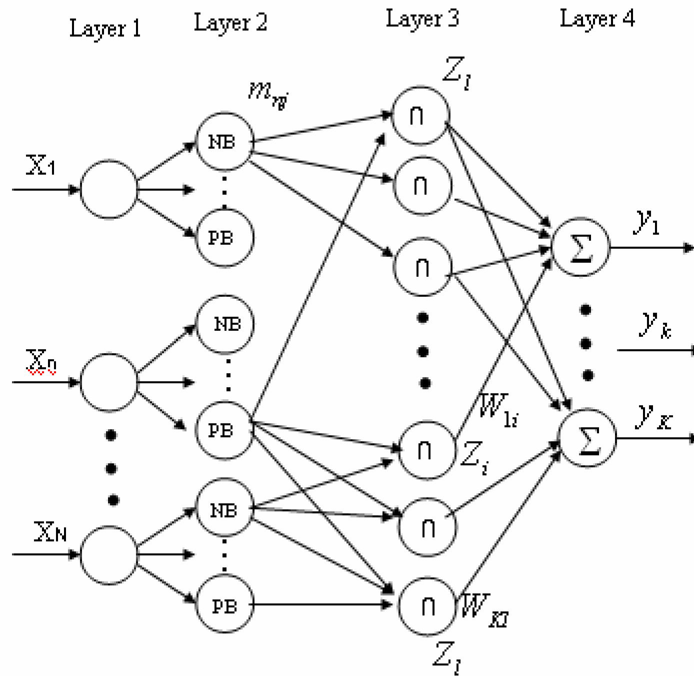

Figure 3.6 Radial basis function based Fuzzy Neural Network

(FNN) structure

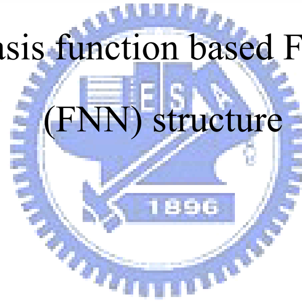

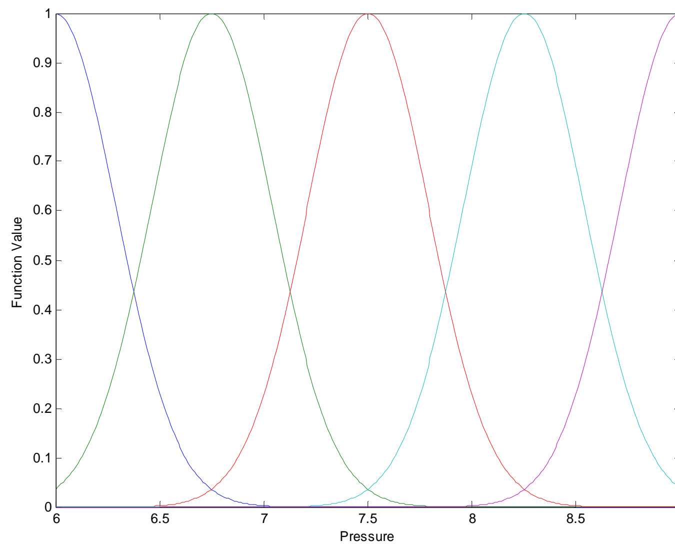

Figure 3.7 The curve of membership function (m=5， α=1.2， β=8.5)

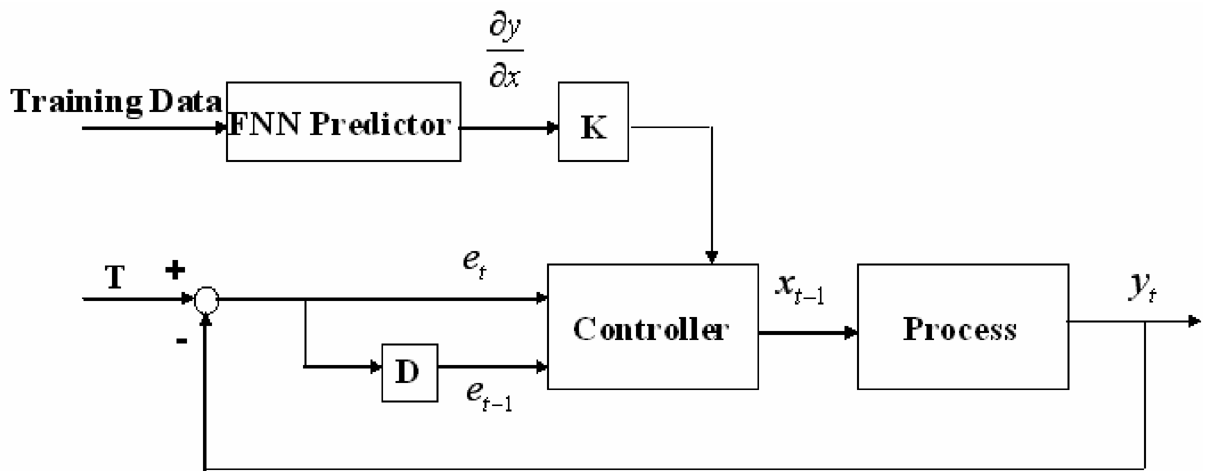

Figure 3.8 Zero error tracking Fuzzy Neural Network (FNN) control block diagram

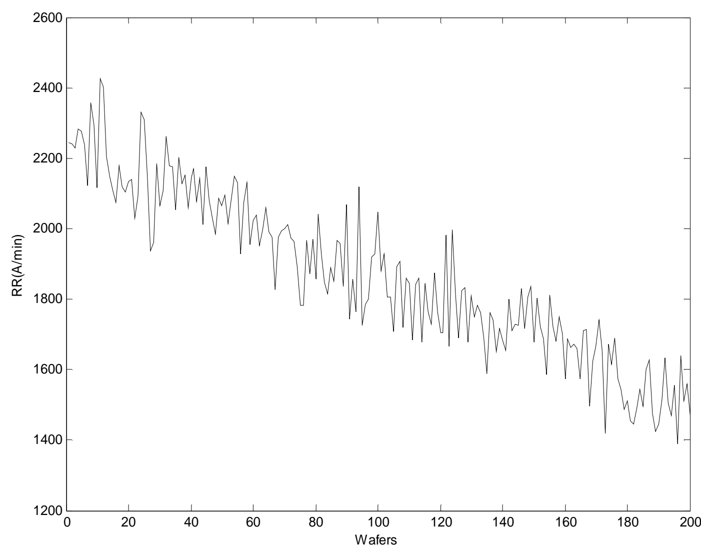

Figure 4.1 Simulation of removal rate variation by Preston Equation

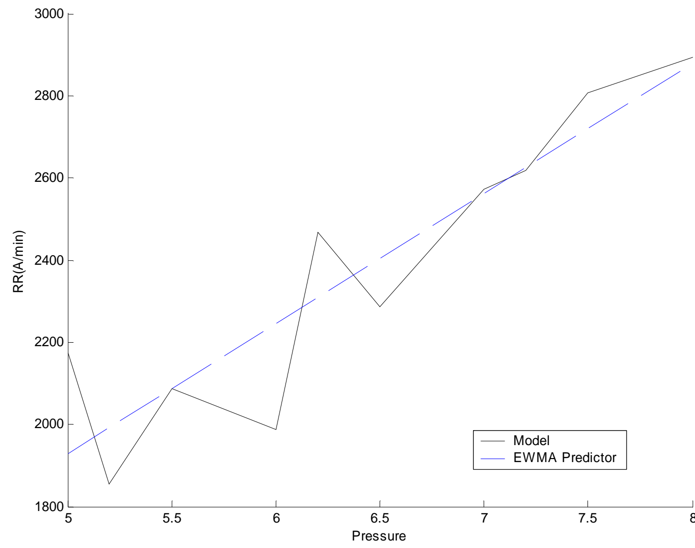

Figure 4.2 Comparisons between the outputs of Preston equation and EWMA predictor

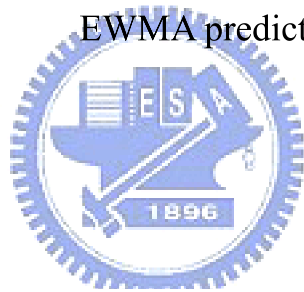

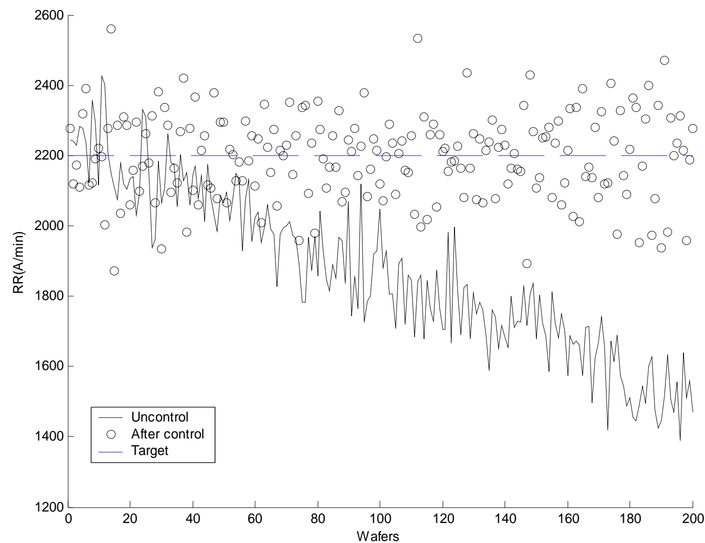

Figure 4.3 Control result of EWMA R2R controller

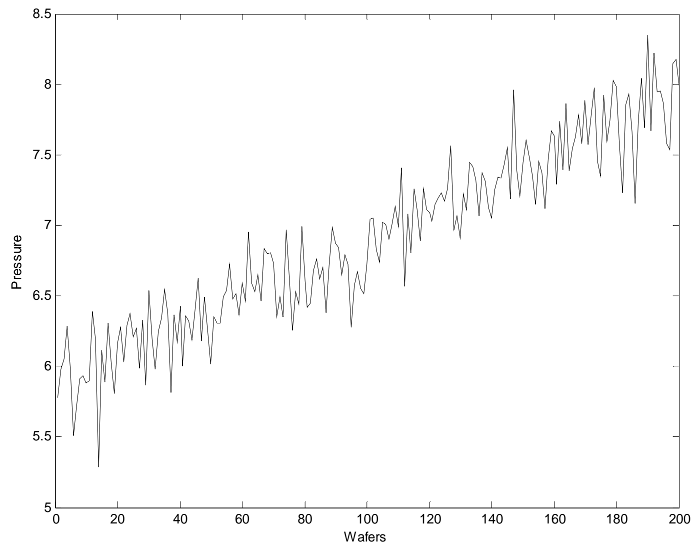

Figure 4.4 The input variation of EWMA R2R controller

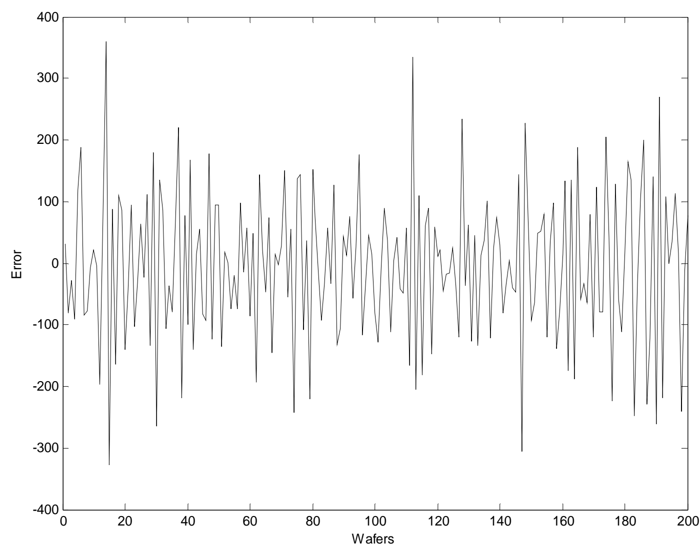

Figure 4.5 The predictive error of each run in EWMA predictor

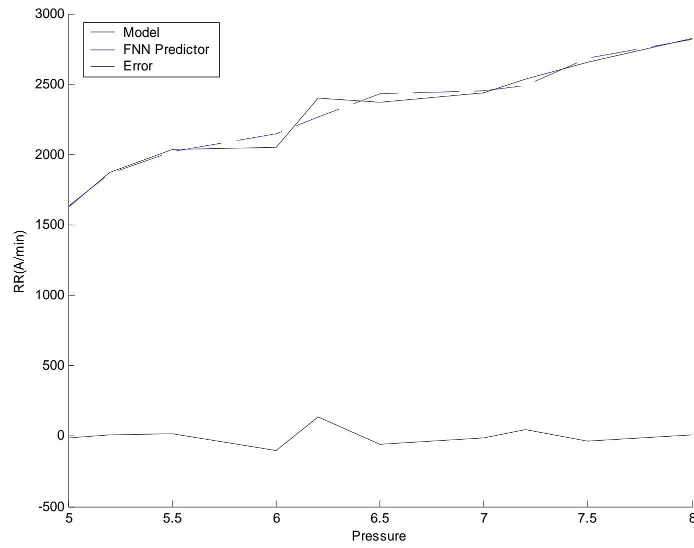

Figure 4.6 Comparisons between the outputs of Preston equation and rough tuning of FNN predictor

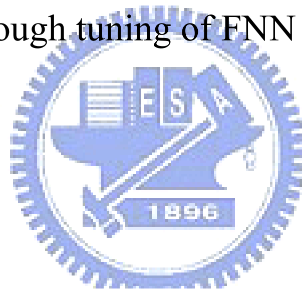

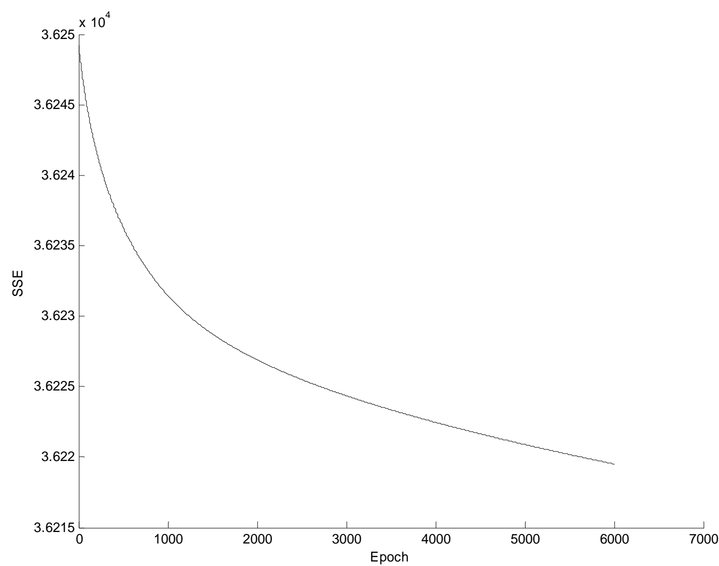

Figure 4.7 The error decreasing trend of fine tuning FNN predictor

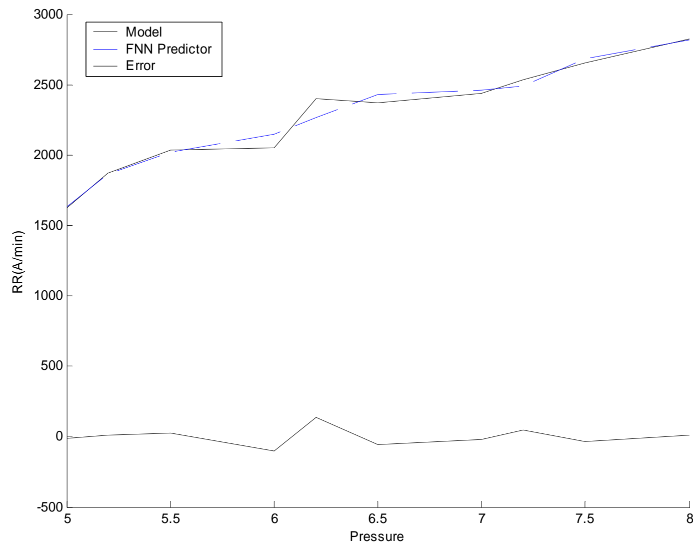

Figure 4.8 Comparisons between the outputs of Preston equation and fine tuning FNN predictor

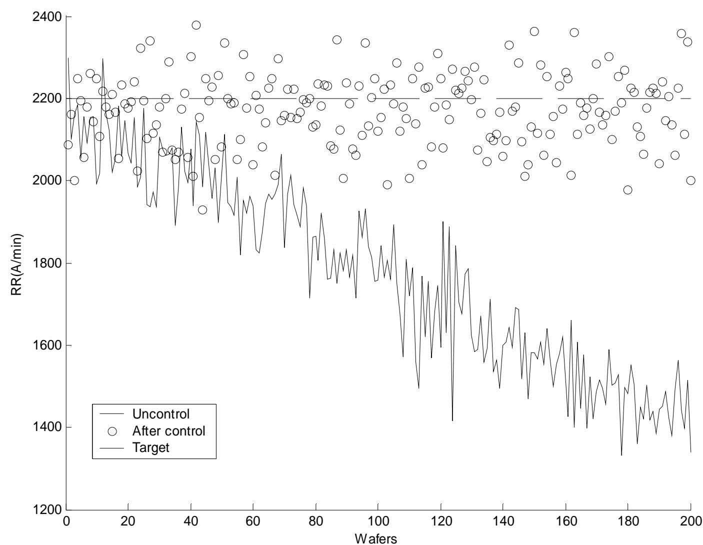

Figure 4.9 Control result of zero error tracking FNN controller

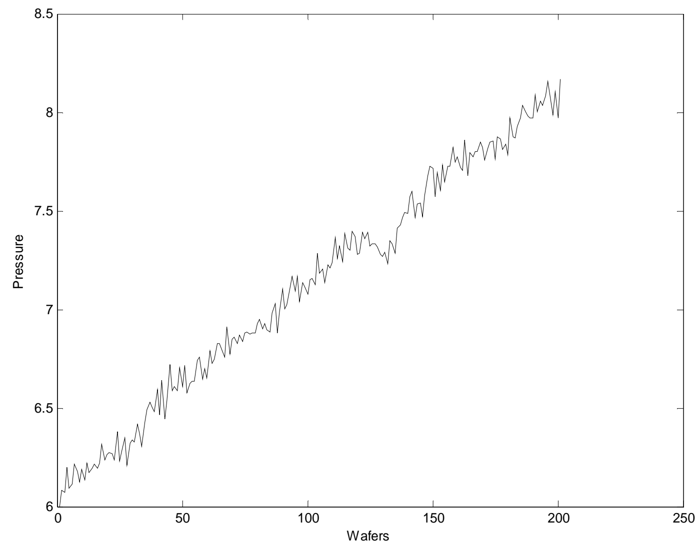

Figure 4.10 The input variation of zero error tracking FNN controller

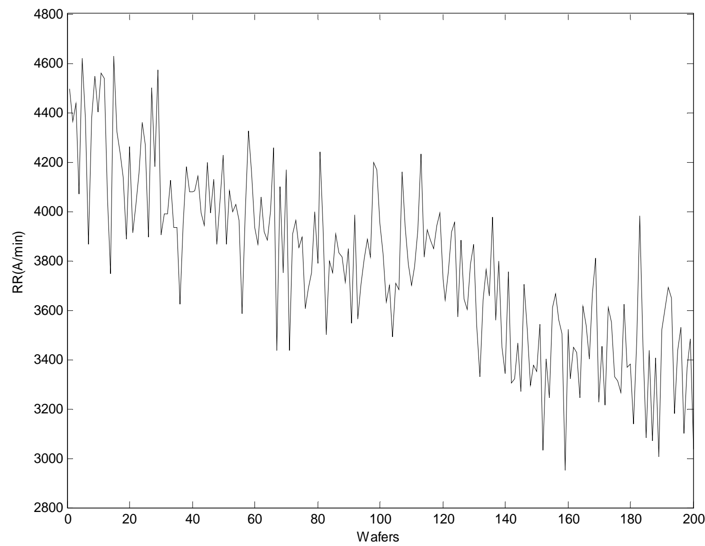

Figure 4.11 Simulation data of removal rate variation by Luo and Dornfeld Equation

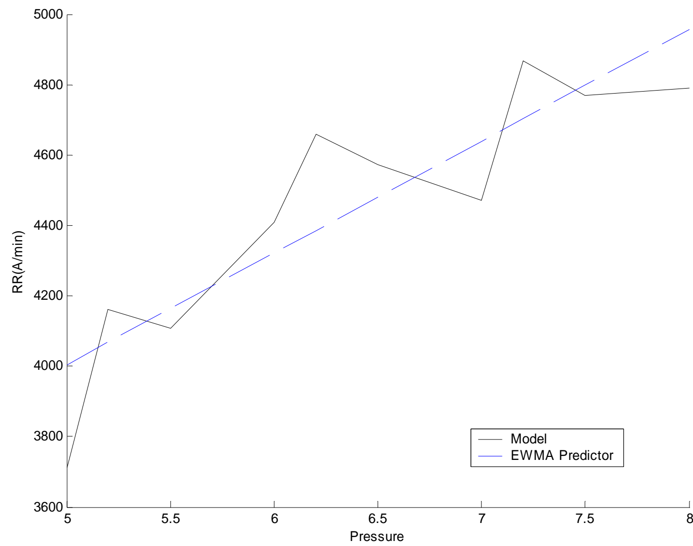

Figure 4.12 Comparisons between the outputs of Luo and Dornfeld equation and EWMA predictor

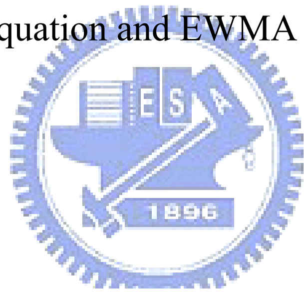

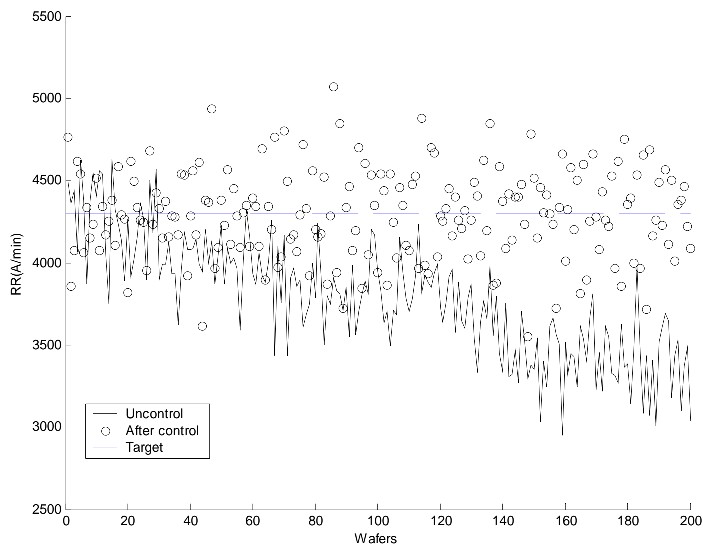

Figure 4.13 Control result of EWMA R2R controller

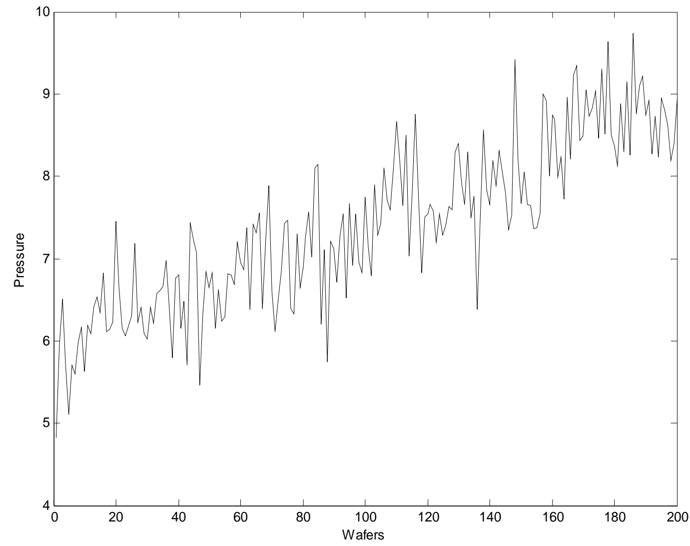

Figure 4.14 The input variation of EWMA R2R controller

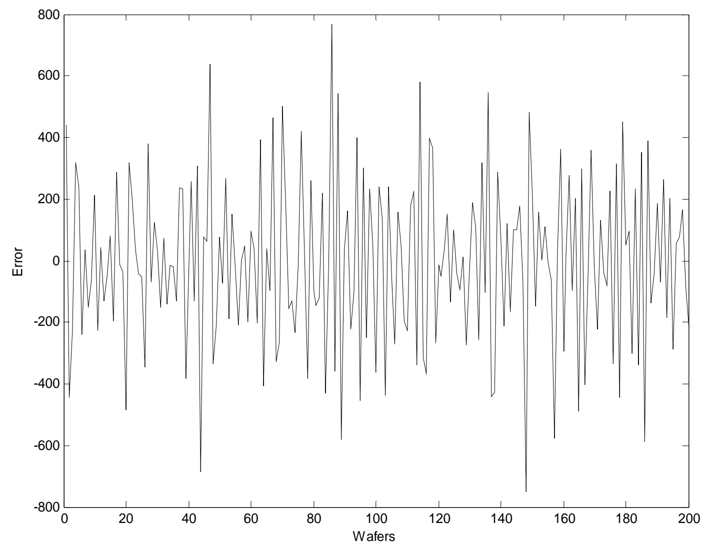

Figure 4.15 The predictive error of each run in EWMA predictor

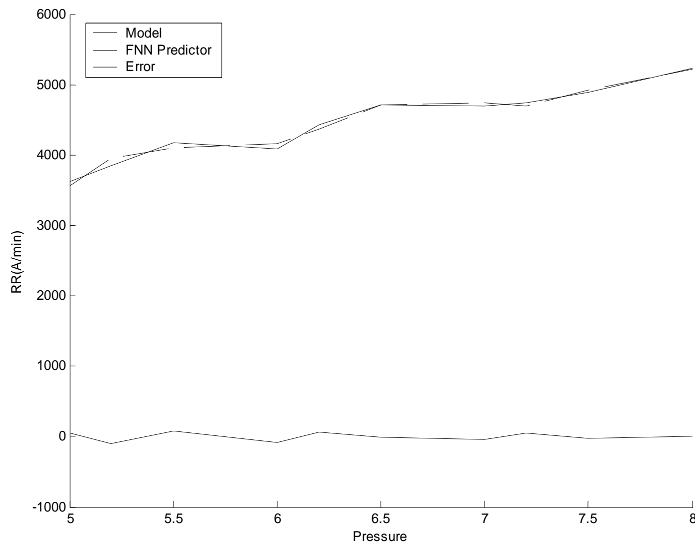

Figure 4.16 Comparisons between the outputs of Preston equation and rough tuning FNN predictor

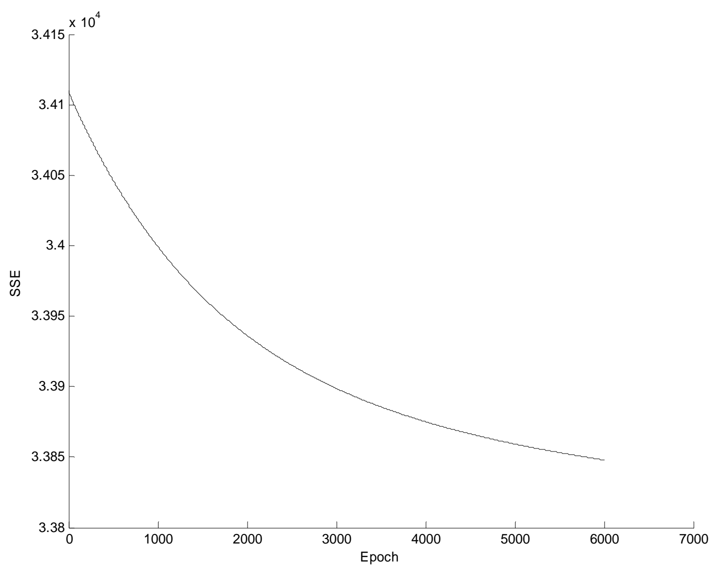

Figure 4.17 The error decreasing trend of fine tuning FNN predictor

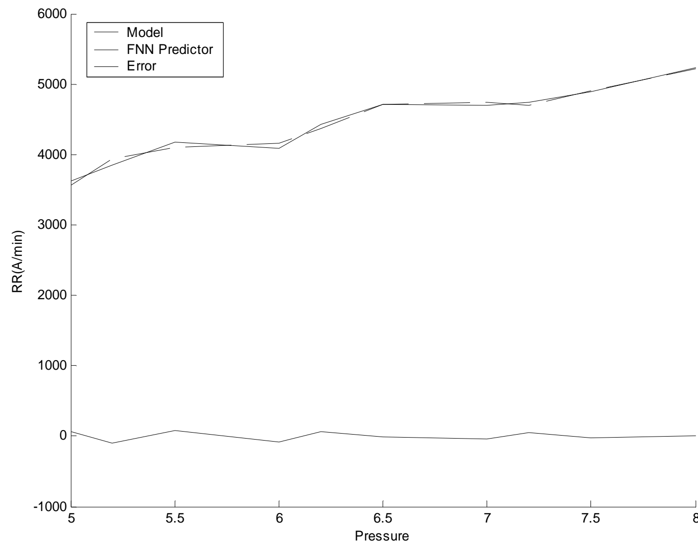

Figure 4.18 Comparisons between the outputs of Preston equation and fine tuning FNN predictor

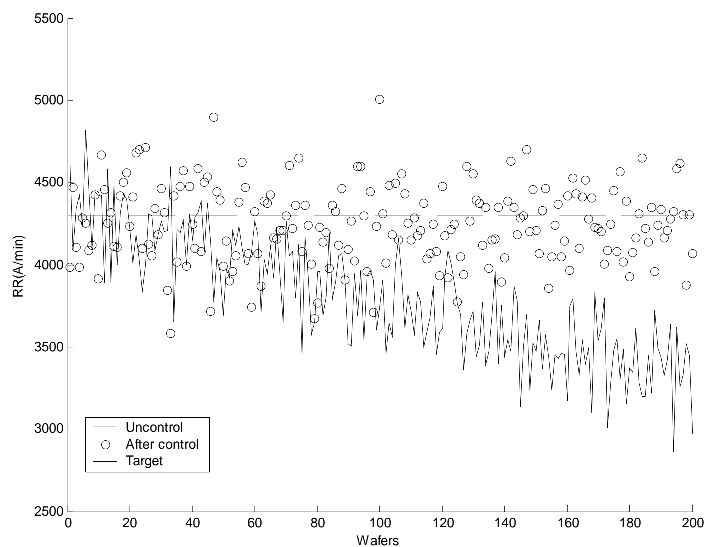

Figure 4.19 Control result of zero error tracking FNN controller

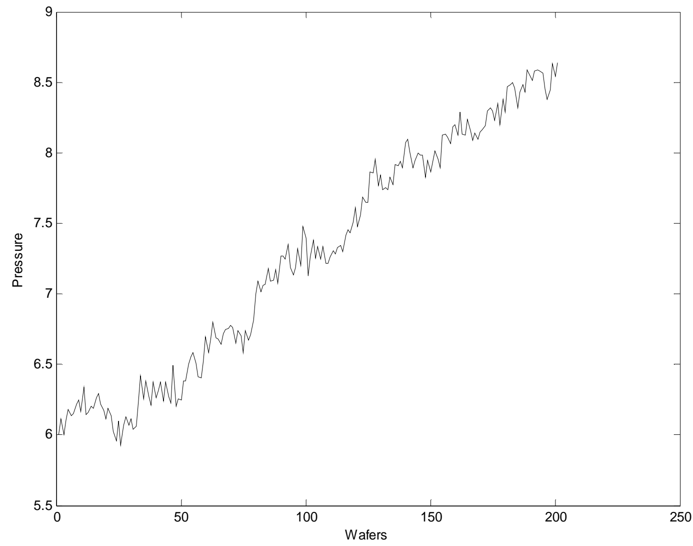

Figure 4.20 The input variation of zero error tracking FNN controller

Figure 5.1 EES Box [29]

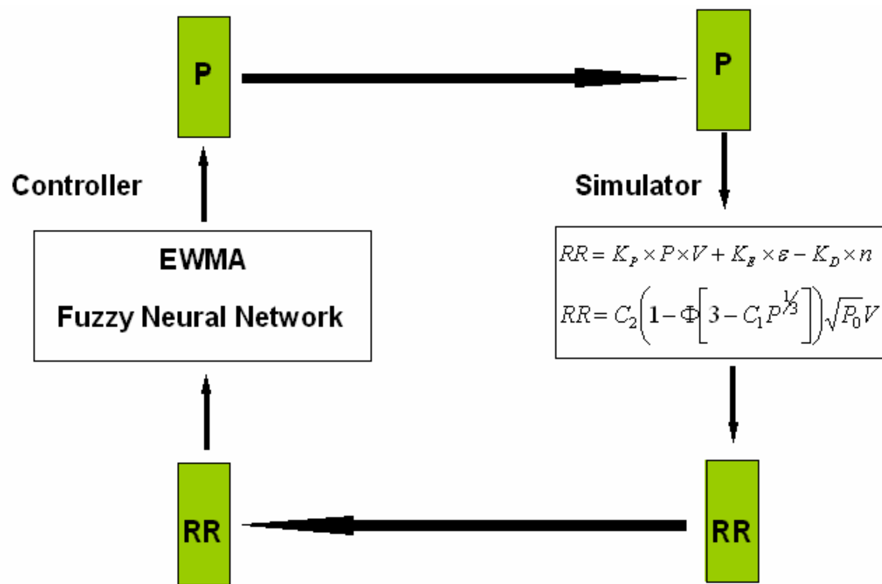

Figure 5.2 The framework of simulator and controller

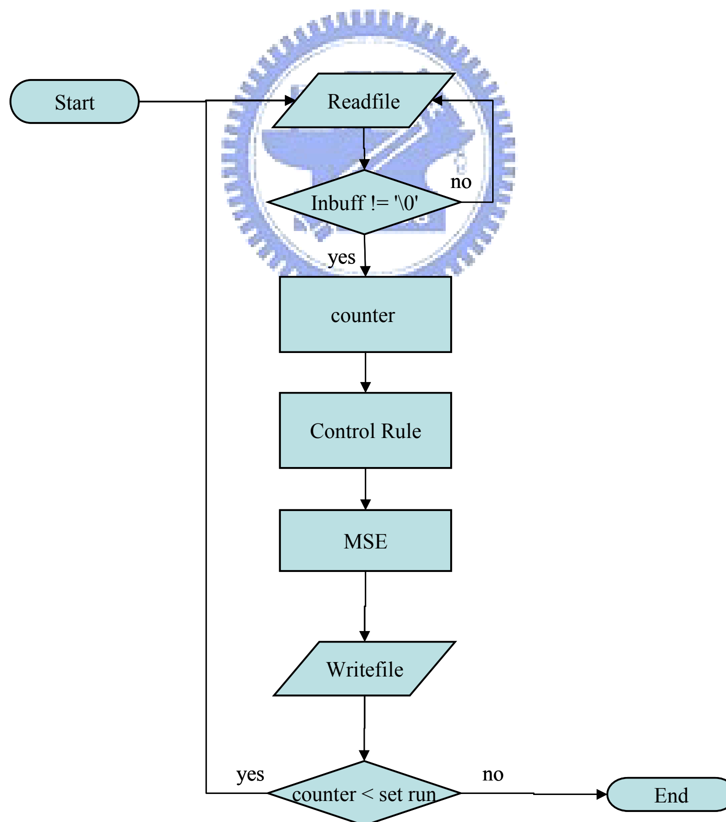

Figure 5.3 Program design flowchart of Simulation Run Mode (Controller)

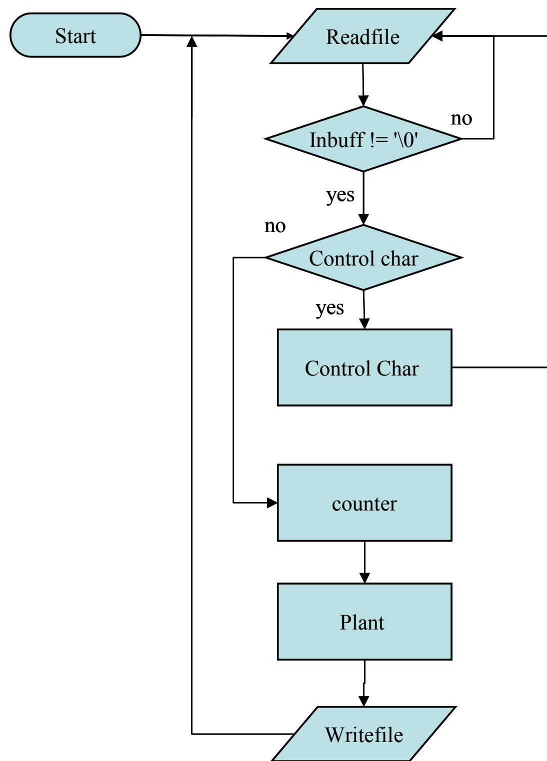

Figure 5.4 Program design flowchart of Simulation Run Mode (Simulator)

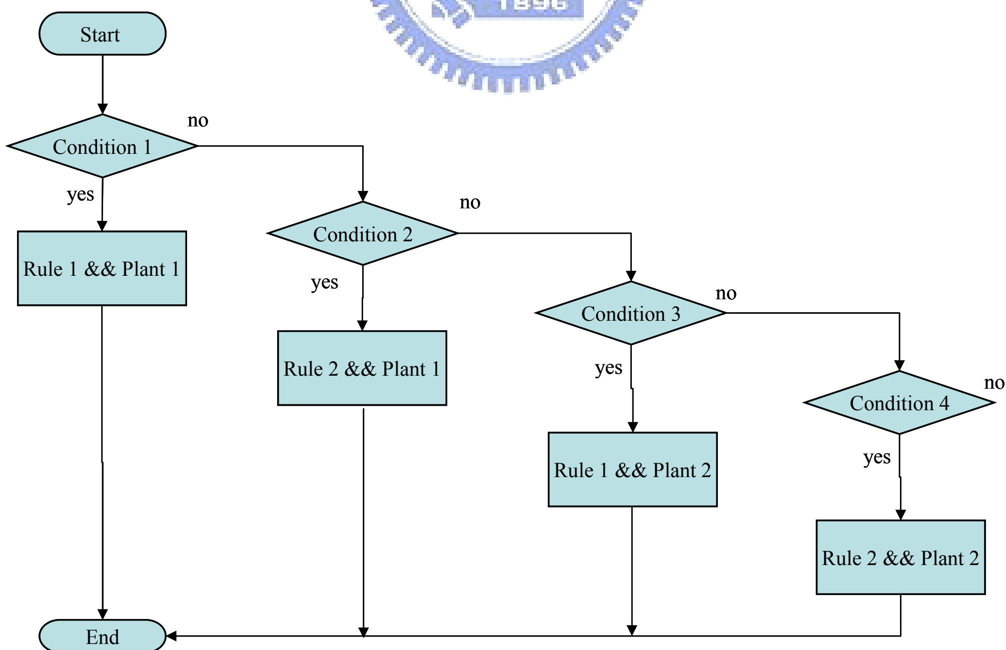

Figure 5.5 Program design flowchart of R2R Control Mode

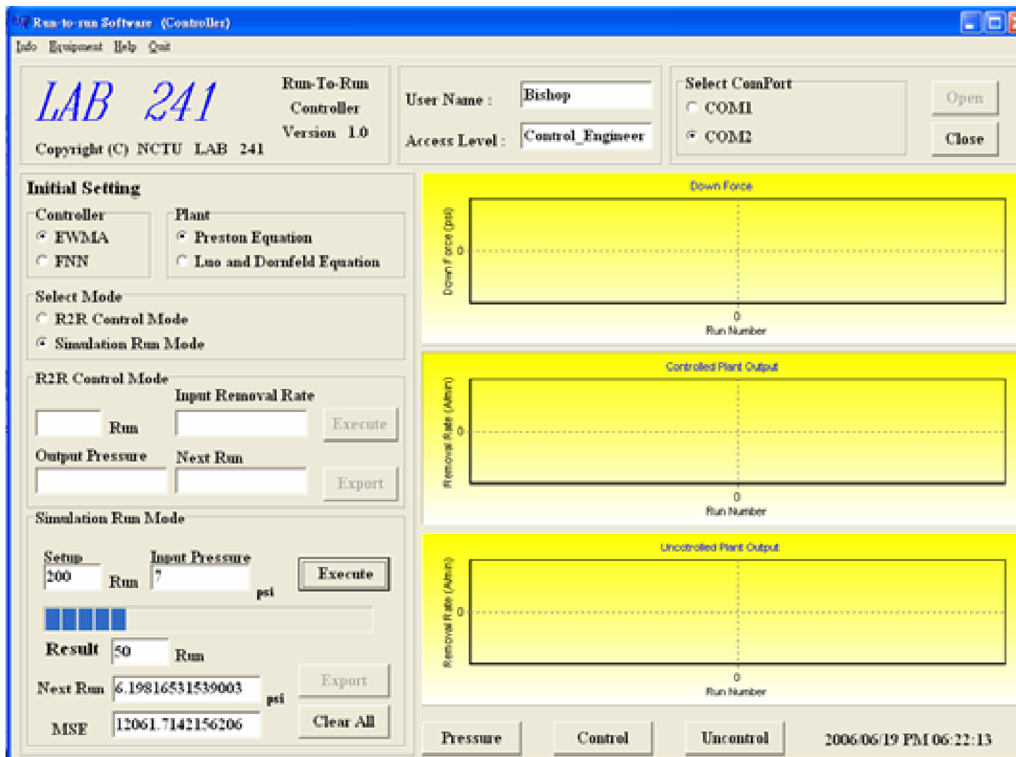

Figure 5.6 The Operator Process Interface (OPI) of the controller

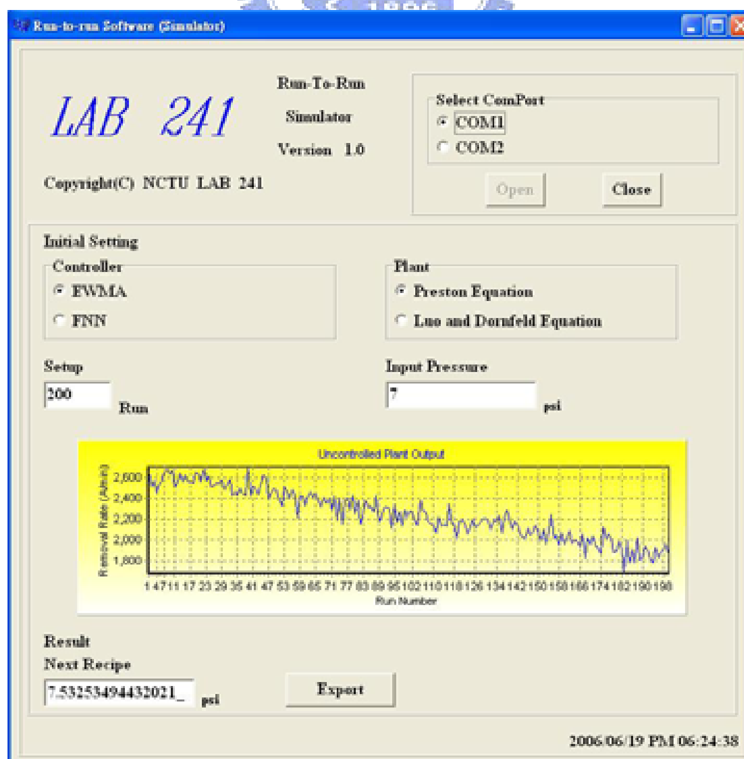

Figure 5.7 The Simulator of CMP Process Equipment

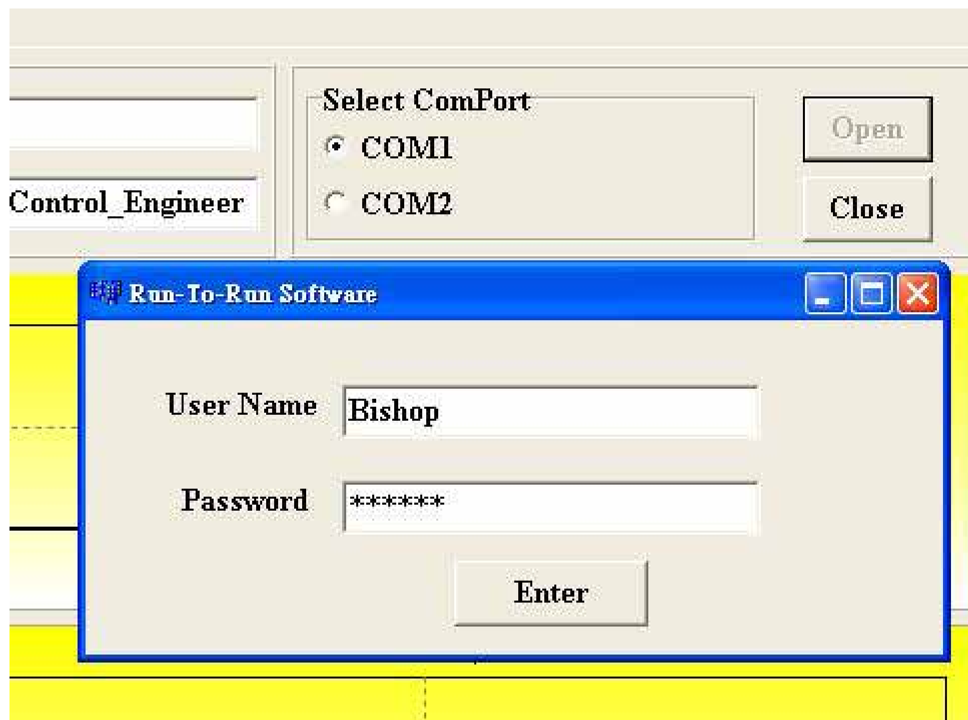

Figure 5.8 The enter frame of the controller

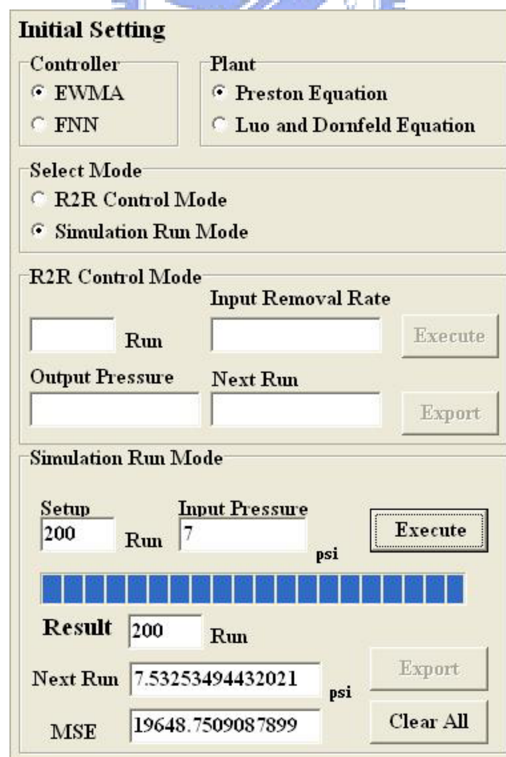

Figure 5.9 The Simulation Run Mode

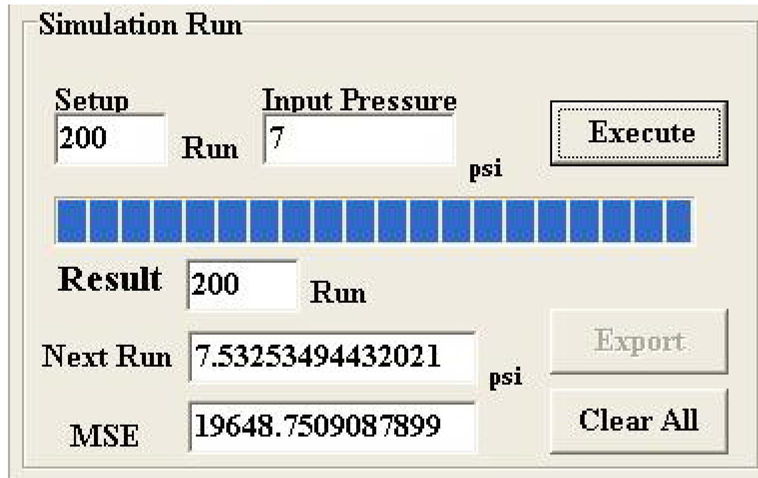

Figure 5.10 The "Result" section of Simulation Run Mode (Controller)

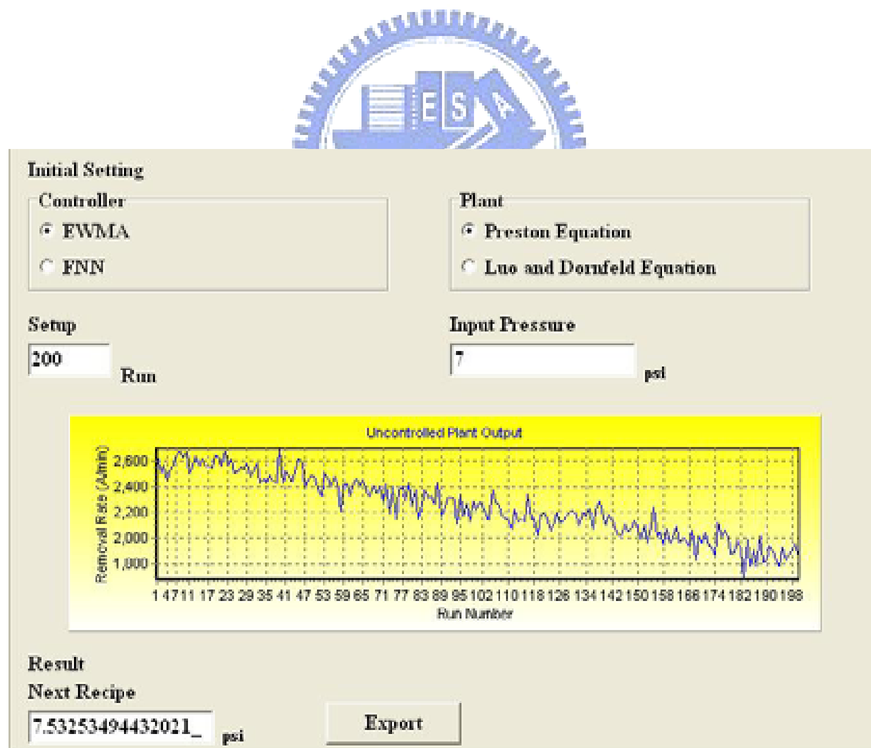

Figure 5.11 The "Result" section of Simulation Run Mode (Simulator)

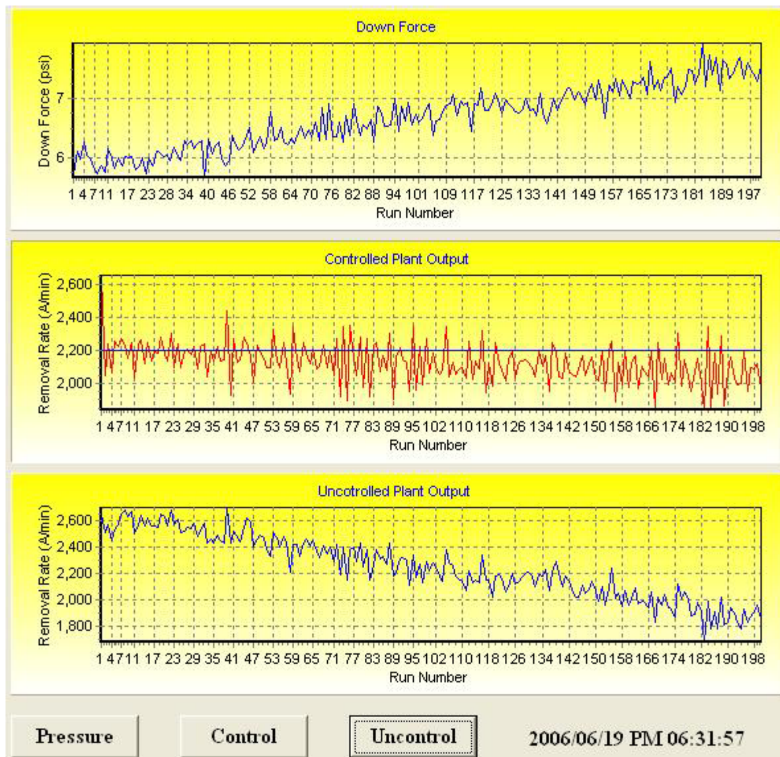

Figure 5.12 The current plots of Simulation Run Mode

Data Export

Run	Control Force	Control	Uncontrol	MSE
1	5.73652898450627	2654.3697344971	2654.3697344971	3929750.18175798
2	6.11727259050557	2043.90972340203	2517.71135421298	1964075.09007099
3	5.97008338028325	2242.10741226933	2573.13018779974	1309916.72725266
4	6.25671572570021	2064.70427427953	2450.92300667331	982437.545439496
5	6.04705413828134	2257.27930062772	2536.01090349014	785950.036351596
6	5.96475356337394	2219.80173211907	2577.15643026357	654958.36362633
7	5.70083700572368	2268.09211619074	2656.30952992551	561392.883108203
8	5.72737824642239	2233.31439882328	2687.5005216769	491218.772719748
9	5.86033610242978	2153.41622122846	2630.64937882007	436638.90908422
10	5.7439114254603	2251.15461615932	2678.52857774815	392975.018175798
11	6.14672664913703	2033.57917290313	2504.61238835552	357250.016523453
12	[illegible]	[illegible]	[illegible]	[illegible]

Display SaveAs Close

Figure 5.13 Export data

Initial Setting

Controller
EWMA
FNN

Plant
Preston Equation
Luo and Dornfeld Equation

Select Mode
R2R Control Mode
Simulation Run Mode

R2R Control Mode
100 Run
Input Removal Rate
2300
Execute
Output Pressure
6.64128951890759
Next Run
2099.78678442632
Export

Figure 5.14 The R2R Control Mode

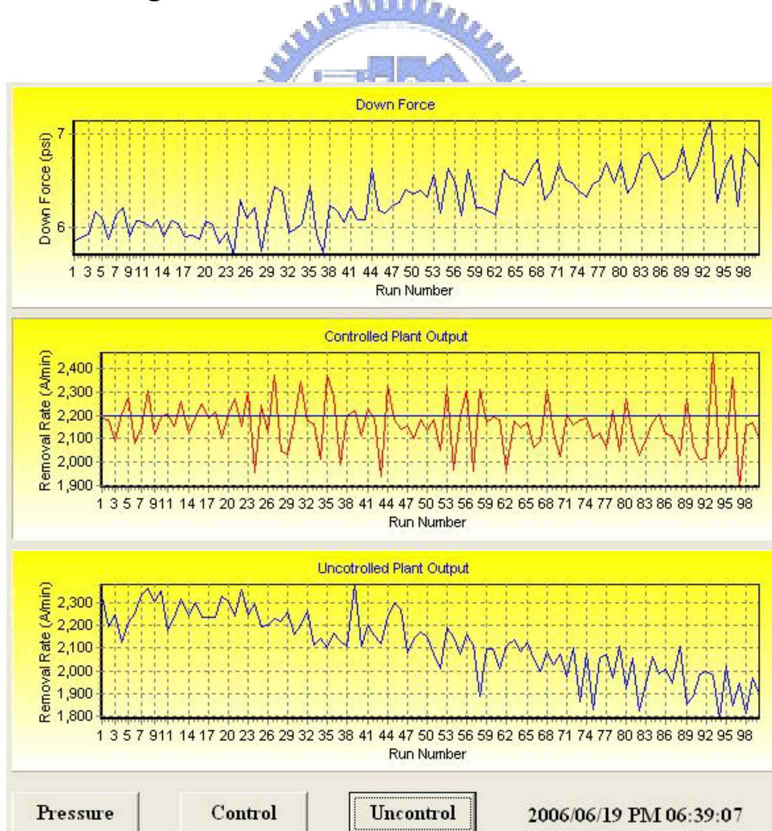

Figure 5.15 The current plots of R2R Control Mode

- Achieves global planarization.
- Universal or materials insensitive–all types of surfaces can be planarized.
- Useful even for multi-material surfaces.
- Reduces severe topography allowing for fabrication with tighter design rules and additional interconnection levels.
- Provides an alternate means of patterning metal (e.g., damascene) eliminating the need of the reactive ion etching or plasma etching for difficult-to-etch metals and alloys.
- Leads to improved metal step coverage (or equivalent).
- Helps in increasing reliability, speed and yield (lower defect density) of sub-0.5 μm devieces/circuits.
- Expected to be a low cost process.
- Does not use hazardous gases in dry etching process.

Table 2.1 Advantages of CMP [18]

- Slurry Chemicals
    - pH
    - Buffering Agents
    - Oxidizers
    - Complexing Agents
    - Concentration
    - Dielectric Constant
    - Slurry Abrasive
    - Type
    - Size
    - Concentration
    - Isoelectric point (pH)
    - zeta potential
    - Stability of the Suspension
- Slurry Flow Rate
    - Transport Under the Wafer
- Temperature
- Pressure
- Velocity
    - Pad
    - Wafer
- Frictional Forces/Lubrication
- Pattern Geometries
    - Feature Size
    - Pattern Density
- Pad
    - Fiber Structure, Height
    - Pore Size
    - Compressibility
    - Elastic and Shear Modulus
    - Hardness
    - Thickness
    - Embossing or Perforations
    - Conditioning
    - Aging Effects
    - Chemical Durability/Reactivity
- Wafer Curvature
- Wafer Mounting
- Film Stack
- Film Stress
- Film Hardness
    - Creep
    - Work Hardening, Fatigue
- Film Microstructure
- Wafer Cleaning Sequence
- Wafer Size

Table 2-2 The Parameters of CMP Process [18]

Specifications

Controller	
CPU	PentinumIII850 above
Storage	HDD 40GB above
RS232	Up to 4 ports
USB	USB2.0 Up to 4 ports
Ethernet	Up to 2 ports
LPT	SPP/ECP
OS	Windows2000 professional

Peripheral	
DI	Isolated X 6, Up to 16
DO	Isolated X 4, Up to 16
AI (optional)	S.E. X 16, Up to 32 or Diff. X 8, Up to 16
Extension	Remote DI/DO/AI/AO available
Power	IN:AC110V/1A, OUT:DC24/1A
Dimension	359 X 180 X 146 (LXWXH, mm)

Table 5.1 The specification for the EES Box [29]

Reference:

[1] M Sarfaty, A Shanmugasundram, A Schwarm, J Paik, J Zhang, R Pan, M J Seamons, H Li, R Hung, S Parikh, "Advanced Process Control Solutions for Semiconductor Manufacturing," *IEEE/SEMI Advanced Semiconductor Manufacturing conference*, pp.101-106, 2002.

[2] James Moyne, "Making the move to fab-wide APC," *Solid State Technology*, pp.72-76, September, 2004.

[3] 蔡嘉鴻，李正一，楊昌霖，"半導體設備工程資料收集技術探討"，機械工業雜誌，第 247 期，pp35-44，民國 92 年 10 月。

[4] 詹玉麒，"快速熱處理之即時模擬器與控制系統"，國立交通大學電機與控制工程學系，碩士論文，2000。

[5] David Maclay, "Simulation gets into the loop," *IEE Review*, Vol. 43, Issue 3, pp109-112, May 1997.

[6] S. Raman, N. Sivashankar, W. Milam, "Design and implementation of HIL simulators for powertrain control system software development," *IEEE Control Conference*, pp709-713, June 1999.

[7] Wojciech Grega, "Hardware-in-the-loop simulation and its application in control education," *IEEE Frontiers in Education Conference*, 12b6-7-12b6-12, November 1999.

[8] Harald Schludermann, "Hardware-in-the-loop-based verification of controller Software," *IEEE Simulation Conference*, pp893-899, Nov. 2000.

[9] 張耀仁, 曹永誠， "Run-to-Run 控制法則分析與比較"， 機械工業雜誌，第 258 期，pp200-205，民國 93 年 9 月。

[10] A.Hu, E. Sachs, and A. Ingolfsson, "Run by run process control: Performance benchmarks," *IEEE/SEMI Int'l Semiconductor Manufacturing Science Symposium,* pp73-78, 1992.

[11] A. Chen and R.-S. Guo, "Aged-based double EWMA controller and its application to CMP process," *IEEE Trans. Semiconductor Manufact.*, vol. 14, pp. 11-19, Feb. 2001.

[12] N. S. Patel, G. A. Miller, C. Guinn, A. C. Sanchez, and S. T. Jenkins, "Device dependent control of chemical-mechanical polishing of dielectric films," *IEEE Trans. Semiconductor Manufact.*, vol. 13, pp. 331-343, Aug. 2000.

[13] D. Boning, W. Moyne, T. Smith, et. al., "Run by run control of Chemical-Mechanical Polishing," *IEEE/CPMT Int'l Electronics Manufacturing Technology Symposium*, pp81-87, 1995.

[14] Z. -C. Lin and C.-Y. Liu, "Application of an adaptive neuro-fuzzy inference system for the optimal analysis of chemical-mechanical polishing process parameters," *Int. J. Adv. Manufactur. Technol.*, vol. 18, no. 1, pp20-28, 2001

[15] J. Yi, Y. Sheng, C. S. Xu, "Neural network based uniformity profile control of linear chemical-mechanical planarization," *IEEE Trans. Semiconductor Manufact.*, vol. 16, No. 4, pp609-620, NOV., 2003.

[16] Ernest J. Wood,"An Object-Oriented SECS Programming Environment," *IEEE TRANSACTIONS ON SEMICOND UCTOR MANUFACTURING ,* Vol. 6. NO. 2, pp.119-127, MAY 1993.

[17] L. Da, V. G. Kumar, W. K. Ho, A. See, et. al., "Run-to-run process control for chemical mechanical polishing in semiconductor manufacturing," *IEEE International Symposium on Intelligent Control*, pp740-745, Oct., 2002.

[18] Joseph M. Steigerwald, Shyam P. Murarka, Ronald J. Gutmann., "Chemical mechanical planarization of microelectronic materials," New York: John Wiley & Sons, 1997.

[19] 李永洲，"化學機械平坦化之最佳化操作：動態規劃法"，碩士論文，國立交通大學機械工程研究所，2004。

[20] F. W. Preston, "The Theory and Design of Plate Glass Polishing Machines," *J. Soc. Glass Tech.*, Vol.11, pp.214-247, 1927.

[21] Luo and D. A. Dornfeld, "Material removal mechanical in chemical mechanical polishing: Theory and modeling," *IEEE Trans. Semiconduct. Manufact.*, vol.14, pp. 112-113, May 2001.

[22] 徐明照、曹永誠，"Run-to-run control 簡介與 APC framework 架構設計"，機械工業雜誌，第 258 期，pp191-199，民國 93 年 9 月。

[23] SEMI E4-0301, "SEMI Equipment Communications Standard 2 Message Transfer (SECS-I)," 2002.

[24] James Moyne, Arnon Max Hurwitz, Enrique Del Castillo, "Run to Run Control in Semiconductor Manufacturing," Boca Raton, FL : CRC Press, 2001.

[25] G. J. Wang, C. H. Yu, "Developing a neural network-based run-to-run process controller for chemical-mechanical planarization," *Int J Adv Manuf Technol*, 2005.

[26] 薛木坤，"應用模糊類神經網路於銅膜化學機械研磨之批次製程控制"，碩士論文，國立交通大學機械工程研究所，2004。

[27] G. J. Wang, J. L. Chen, J. Y. Hwang, "New Optimization Strategy for Chemical Mechanical Polishing Process," *the JSME International Journal*, Series C., Vol.44, No.2, pp534-543, 2001

[28] C.T. Lin, C.S.G. Lee, “Neural fuzzy systems: a neuro-fuzzy synergism to intelligent systems,” Upper Saddle River, NJ: Prentice Hall PTR, c1999

[29] http://www.secs.itri.org.tw/